Article

An Advanced Energy-Efficient Environmental Monitoring in Precision Agriculture Using Lora-Based Wireless Sensor Networks

Višnja Križanović [1,*], Krešimir Grgić [2], Josip Spišić [3] and Drago Žagar [4]

[1-4] Josip Juraj Strossmayer University of Osijek, Faculty of Electrical Engineering, Computer Science, and Information Technology
* Correspondence: visnja.krizanovic@ferit.hr

Abstract: Sensor networks, as a special subtype of wireless networks, consist of sets of wirelessly connected sensor nodes often placed in hard-to-reach environments. Therefore, it is expected that sensor nodes will not be powered from the power grid. Instead, sensor nodes have their own power sources, the replacement of which is often impractical and requires additional costs, so it is necessary to ensure minimum energy consumption. For that reason, the energy efficiency of wireless sensor networks used for monitoring environmental parameters is essential, especially in remote networking scenarios. In this paper, an overview of the latest research progress on wireless sensor networks based on LoRa was provided. Furthermore, the analyses of the energy consumption of sensor nodes used in agriculture to observe environmental parameters were carried out. Optimization methods of energy consumption, in terms of choosing the appropriate data collection processes, as well as the settings of wireless network radio parameters were suggested. In the conducted analyses, special emphasis was placed on choosing the optimal package size. In this paper, it was proven that the adjustment of the transmission speed to the actual size of the packet is important for better energy efficiency of communication.

Keywords: LoRa technology, Wireless Sensor Networks, Energy Efficiency, Environmental Monitoring, Precision Agriculture

1. Introduction

Sensor networks consist of a group of wirelessly connected sensor nodes used for gathering and exchanging information. The collected data are forwarded from sensor nodes via gateways to public or private servers [1] for easier data access and processing [2]. In this case, the data do not have to be forwarded to central locations but they can be stored and processed on local servers. Given that sensor nodes can be equipped with various types of sensors, the field of application of wireless sensor networks is very broad. One of the many possible areas of usage of wireless sensor networks within the Internet of Things (IoT) ecosystem includes their application in agriculture and monitoring of environmental parameters [3] - [8]. In this case, the environment consists of agricultural crops for which environmental and other parameters essential for yield prediction are observed under different conditions.

The broad usage of microprocessors and microcontrollers, which include small sensor nodes that can be self-modifiable, low-cost tooling, and scalability, demonstrates that wireless sensor networks can be used in the digitization of agriculture [9]. Wireless systems based on the usage of sensor nodes make processes in agriculture more intelligent because they become more precise, data-oriented, and greatly automated [10].

As they join a large number of sensor nodes into a network, wireless sensor networks represent the base for an extremely heterogeneous IoT environment in which there are many different technologies and communication standards. Such heterogeneous

 doi:10.20944/preprints202306.1057.v1

environment enables optimal adjustment to different areas of sensor application. Every field of application requires a suitable selection of communication systems and parameters to achieve reliable and energy-efficient communication.

The research activities carried out in this paper are set to the application of wireless sensor networks in agricultural development based on the collection and processing of environmental data. Therefore, the specifics related to the application of sensor networks for digital agriculture are considered. Scientific research into environmental and agronomic parameters essential for crop production is aimed at coping with and/or mitigating the increasingly severe consequences of climate change, which will continue to intensify.

Activities related to the efficient application of wireless sensor networks in agricultural processes contribute positively to the sustainable development of the economy based on agriculture and food production. The effects of these activities also have a positive impact on the ecology. The processes of monitoring ecological and agronomic parameters that enable a precise assessment of the physiological state of crops enable the timely adjustment of agrotechnical measures to reduce the impact of climate change on agricultural production.

The aim of the implementation of wireless sensor networks in test environments is to connect sensor nodes, deployed at different remote locations, to servers used to store and process data in a reliable and energy-efficient manner. To enable applied research aimed at increasing the efficiency of implemented wireless sensor networks, the communication processes that occur within the networks are subjected to testing for the selected scenarios. The analyses include the specifics of communication in different scenarios regarding the need for continuous monitoring of network parameters and real-time communication.

When defining the periods in which communication aimed at collecting data from the environment should occur, it is necessary to consider how frequently communication processes should occur. This depends on the appropriate sampling period and the number of samples that are required for data processing and analysis based on which plant treatment procedures can be defined. Then, based on the conclusions of the sample analyses, in case of deviation from the optimal conditions, it is possible to implement stress protection measures that include watering or feeding the plants.

It is necessary to analyze the specifics of communication processes in different scenarios, for instance, those regarding the locations of the implemented sensors and the settings of network communication parameters. Within this process it is imperative to analyze the behavior of the implemented wireless sensor network in real conditions, based on which the optimization of communication processes among sensor nodes is possible. Optimization can be carried out, for instance, regarding network topology, location of nodes, and methods of data collection.

The source of energy required for the activities of the sensor nodes is primarily a battery. The sensor nodes can operate from several months up to several years. According to some laboratory testing within the IoT field by authors of [11], the internal battery can operate for more than four months without an additional power source. The total life cycle of the sensor node battery is limited. The batteries, such as Lithium-ion batteries, are sensitive to capacity fading over a final number of cycles.

According to [12], the term "life cycle" specifies the lifetime of a battery in the number of cycles to reach 80% of the estimated battery capacity. The entire life cycle of the battery involves both the cycle of operation and inactive storage operations. The battery cycle is affected by numerous different stress factors including temperature, discharge current, charge current, and state of charge ranges. Furthermore, inactive storage of batteries also reduces their capacity. Battery degradation during storage is affected by the battery's state of charge and temperature. Over their lifespan, batteries degrade gradually. This, as well as a variety of chemical and mechanical changes on the electrodes, leads to reduced capacity.

The finite life cycles of sensor node batteries represent a major operational constraint. One of the methods to overpower this limitation is the energy harvesting process. There

 doi:10.20944/preprints202306.1057.v1

are currently many available energy sources, but solar energy is flexible, mature, and presents an external power source. A sensor node's battery can be connected to a solar collector as a supplementary system for its charging, so with solar power, the working life of the sensor node battery is extended.

With or without additional solar power, the battery has a limited operating life and after that it needs to be replaced. With respect to the placement of the sensor node, replacing the battery is often impossible or impractical. Considering the disposition associated with battery replacement, the methods related to increasing efficiency and reducing energy consumption are essential with or without solar power.

Since the sensor node's battery life cycle is one of the most severely limited resources in the network, for the implementation of the wireless sensor network, it is important to consider the optimization of energy consumption and to achieve the maximum possible energy savings. Therefore, in this paper, the configurations of wireless sensor networks concerning the optimization of the consumption of energy are analyzed. Optimization is analyzed in terms of the choice of adequate topology, node layout, data collection, as well as the set-up of network radio parameters.

The content and contributions of the paper are outlined in the following way: In Section II, applications of wireless sensor networks in precision agriculture are described. In Section III, an overview of issues related to the energy efficiency of LoRa sensor networks is presented. In Section IV, the energy consumption model of LoRa sensor node is presented. In Section V, wireless communication parameters in LoRa networks are defined, the selection of adequate parameters for LoRa-based communication is clarified, aspects of wireless communication based on LoRa have been analyzed regarding the choice of the appropriate volume of traffic in the LoRa network, the structure and format of the LoRa packets, the constraints based on LoRa time-on-air communication, as well as both unconfirmed and confirmed data transfer processes. Finally, in Section VI, the evaluation and the optimization of energy consumption in LoRa sensor networks are analyzed in detail in selected scenarios; in Section VII the results are presented; and in Section VIII, the most important concluding remarks related to the selection of solutions that provide adequate energy efficiency of LoRa-based communication are highlighted.

2. Environmental Parameters Monitoring in Precision Agriculture Using Wireless Sensor Networks

Extreme weather conditions due to climate change and the shift to organic farming pose new challenges for crop production in Europe and the rest of the world [11]. The challenges of climate change present a major threat to crop growth and food production. Crop production is particularly receptive to extreme weather conditions, especially in the growing season. Therefore, it becomes essential to monitor both the crops and the environment to make adequate agricultural arrangements at an adequate time based on the current situation in the field [11].

Within the IoT-based ecosystem, the application of various IoT devices enables continuous monitoring of changing environmental conditions. Measuring local weather impacts on crop yield with accuracy is possible with wireless all-in-one weather stations, i.e., sensor nodes equipped with specialized sensor boards, which integrate different sensors, while satellites and drones extend monitoring to areas not covered by IoT devices to provide remote sensing.

The "smart agriculture" concept, a concept based on the application of IoT solutions in agriculture, can be applied to reduce the risks related to the negative impacts of weather conditions on crop production and to improve agricultural yields, with fewer resources invested [10]. Some of the possible IoT solutions that can be applied in smart agriculture are solutions based on the application of wireless sensor networks. In wireless sensor networks which are implemented in agricultural areas, the sensor nodes are interconnected to collect relevant information from the fields and to forward the collected data to servers for their further processing. IoT-enabled smart agriculture has the potential to achieve

 doi:10.20944/preprints202306.1057.v1

maximum extraction of values from the data since the intended analysis of the data serves in the advancement of the production processes [11]. Data obtained from various sources are stored on servers. Data stored on servers are processed and interpreted to help in decision-making processes.

According to [11], continual and heavy monitoring of environmental and agronomic parameters in the field creates a high volume of data for data-driven agriculture. Data-driven and IoT-enabled agriculture provide circumstances to address the challenges posed to agricultural processes by frequent changes in weather conditions and by the increasingly common occurrence of weather extremes. Moreover, agriculture based on environmental data analysis enables a gradual transition to organic farming by enabling the opportunity to reduce the commonly used inputs required for crop growth. It can be considered a promoter of the strategic goals of the EU's strategies for organic agriculture, which should be achieved by 2030.

Moreover, IoT solutions bring major improvements to the agricultural sector, as the processes of data collection, processing, and analysis become highly automated. Different types of wireless sensor nodes distributed in the field enable the collection of related data in real time, with continuous soil and crop monitoring. Distant monitoring of environmental and agronomic parameters is carried out in all stages of the production process, from soil preparation and sowing to harvesting [3] - [7]. For this purpose, the sensor nodes may be equipped with a specialized sensor board that integrates a large number of various sensors, depending on a particular field of application, and adapted to different types of environments or crops. In this way, sensors intended to control the cultivation of agricultural crops can monitor environmental parameters such as air temperature, air humidity, soil temperature, soil moisture, chemicals in the soil, leaf wetness, air flow, insolation, luminosity, and solar radiation.

The operation of wireless sensor networks used in the monitoring of environmental and agronomic parameters is extensively documented in the scientific literature, due to their wide application area. Thus, for example, in [13] - [15], sensors used to observe environmental parameters such as air temperature and humidity are considered, in [16] sensors used to observe the temperature and pH level are considered, in [17] sensors to observe humidity, the speed and direction of the wind, the rain gauge and the amount of water for irrigation are considered, in [18] sensors for observing soil temperature and humidity are considered, while in [19] and [20] observing water management is considered, as well.

The approach known as "precision agriculture", which refers to the application of modern IoT solutions in agricultural activities, is widely accepted since it enables efficient and environmentally friendly agriculture [21]. For instance, it allows for the minimization of the impact of diseases and pests on the yield and consequently reduces the use of pesticides [22]. Based on the principles of precision agriculture, it is possible to ensure the application of adequate agrometeorological measures that help to achieve high-quality yields, proposed considering the specifics of each particular case of application. The most important applications of precision in agriculture relate to processes of monitoring environmental and agronomic parameters, such as temperature and relative humidity of the air or soil. These processes aim to reduce the risks during the production of a certain type of crop, based on the application of appropriate procedures, such as irrigation or fertilization [23], [24].

Explicit and related data obtained from the implemented sensor network are gathered using sensors and forwarded to servers where they are stored in databases and analyzed for optimizing agrotechnical measures [8]. In this way, the agricultural sensor network can radically transform traditional agriculture and turn it from a statistical to quantitative access since it provides access to significant real-time data relevant to making the right decisions related to agriculture by assessing the current conditions and determining the preferred time to apply certain cultivation practices. These decisions include, among other things, the selection of suitable land, response to drought and irrigation, yield optimization, and control of chemicals. Agrochemicals include fertilizers, pesticides, and

 doi:10.20944/preprints202306.1057.v1

herbicides. Thus, significant savings can be achieved by the use of irrigation water, by the use of chemicals, as well as through human labor.

When applying IoT technology for soil analysis, objective information specific to the terrain is obtained, which is related to the state of the soil, such as its humidity, nutrient level, and irrigation level. Accurate soil mapping enables the selection of optimal crop varieties for sowing, which correspond to the chemical, physical, and organic status of the soil, and it also enables the optimal selection of agrotechnical measures when preparing the soil for sowing [10].

Furthermore, when applying IoT technologies in irrigation systems, the efficiency of water use can be significantly improved, which is essential in the context of the growing lack of fresh water caused by changes in climate. Data collected from the field are combined with data about weather conditions to control different types of irrigation systems as well as to achieve optimal water use and better crop quality. Moreover, when applying IoT technology in the analysis of nutrients in the soil, the aim is to obtain precise data on the nutrients necessary for the growth and health of plants, in order for the preparation of the fertilization process to be precisely planned without the excessive use of fertilizers. For this reason, the mentioned concept is also important from an ecological point of view since the extreme use of fertilizers negatively affects the quality of the soil and the environment. Subsequently, when applying IoT technology for real-time monitoring of crop diseases, very precise treatment of plant diseases is enabled, with a significant reduction in the number of pesticides [1]. In addition, IoT technology can be used to monitor yields and forecast the appropriate harvest time for optimal crop quality. For the above reasons, the application of IoT solutions is increasingly common in greenhouses, orchards, and vineyards [25] - [29]. The capability to provide the right data at the right time while incorporating contextual information, has not yet been universally exploited in IoT-enabled agriculture based on collected data. Many early-stage agricultural IoT systems, which mainly focused on the application of individual sensor nodes, failed to come upon the existing demands of agricultural production due to the limited scalability and interoperability of the entire system [11]. For this reason, as a part of the project [30] activities, within which the research activities are carried out and described, the architecture and design of an IoT-based ecosystem for data-driven agriculture are provided. This platform provides effective solutions for continuous collection and remote monitoring of agrometeorological and crop conditions, as well as the integration of different services for analytics and data visualization. For the processes of efficient directing of the collected sensor data to a remote distant destination, optimization is crucial. In order to optimize the parameters of wireless communication, it is necessary to carry out analyses of various communication aspects. Therefore, the optimization of parameters is carried out to achieve reliable communication with minimal energy consumption.

3. Overview of Issues Related to Energy Efficiency of Lora Sensor Networks

3.1. Energy efficiency of LoRa networks

Sensor nodes are characterized by small dimensions and low energy consumption, as well as the ability to collect data via appropriate sensors, to process data, and support wireless communication within the appropriate range. This concept enables the collection of data very close to the observed area, local aggregation of data, and easy transfer of data to remote central locations intended for data storage and processing. Wireless sensor networks may contain some nodes located at relatively short distances from each other. Communication between sensor nodes, as well as communication between sensor nodes and the gateway can occur either directly or through several sensor nodes, within the so-called multi-hop topologies which extend the communication range [31].

For monitoring of environmental and agronomic parameters, sensor networks are placed in remote locations, i.e., agricultural lands. Therefore, it is necessary to use networking technologies that can achieve connectivity over long distances up to several tens of kilometers. For this reason, the application of short-range information and

 doi:10.20944/preprints202306.1057.v1

communication technologies, such as ZigBee and WiFi, is not suitable due to the limitations related to the impossibility of installing additional gateways as a result of the lack of suitable locations or inadequate connection to electricity [32]. Although the deployment of communication via mobile networks meets the requirements on range and reliability, it is energy demanding and incurs additional costs in terms of permanent subscription to the service provider. Hence, it is also not an optimal solution [33].

In addition to being long-range, the next important criterion in the selection of appropriate technologies is low energy consumption, so that the battery-powered nodes achieve a sufficiently long autonomy and multi-year life cycle expectancy. Therefore, technologies from the group of Low Power Wide Area Network (LPWAN) technologies, high-range low-power wireless technologies, are suitable for application in precision agriculture scenarios [34]. The specifics of LPWAN technologies are a long communication range for sending information over greater distances and low power consumption. These features make LPWAN technologies very practical for open-area IoT implementations. There are many LPWAN technologies and new ones are constantly emerging and improving, but currently, LoRa, Sigfox, and Narrowband IoT (NB-IoT) are leaders in the field [35], [36]. The advantage of the application of these technologies in networking relates to the fact that the end devices working with these technologies are designed to consume energy efficiently and minimally [37]. Low power and narrow bandwidth allow for very low power consumption used in operation [38].

Its low power associated with long-range communication makes LoRa the most prominent among LPWAN technologies [39]. Of all LPWAN technologies, LoRa has probably involved consideration of most scientific studies concerning problems, current solutions, and open issues [41] - [62]. A significant number of surveys has been conducted [41] - [50] with the aim of analyzing requirements, deployments, and challenges of LoRa technology. Therefore, available survays [41]-[50] from 2019-2023 are listed and briefly described hereafter. In [40], a systematic literature review of published studies on LoRa applications was conducted using articles from 2010-2019. The study [41] presents an overview of LoRa networking, covering the technological difficulties in setting up LoRa infrastructures, such as connection management, allocation of resources, consistent communications, and security. In [42], a comprehensive survey of LoRa from a systematic perspective is given. It includes analysis of LoRa communication processes, security, and its enabled applications. In [43], the landscape of available simulators for IoT and wireless sensor networks is explored and their performance is compared. Moreover, LoRa networking performance metrics, including range, throughput, energy usage, and security is studied in [44] and [45]. In [46], literature survey presented in the paper describes LoRa performance under different scenarios and few implementation obstacles of this technology. Furthermore, in the papers [47] and [48], the discussion about the advantages of LoRa over the existing technologies used in IoT is presented. Finally, in [49] and [50], a detailed description of the LoRa technology is given with regard to existing security and reliability mechanisms.

The reason for the great number of scientific studies within the field of LoRa deployment can be making clear the cause of the public availability of its specifications [63], the availability of certified hardware [64], and the fact that LoRaWAN communication can be facilitated without necessity to establish a contract with a network operator. The LoRaWAN, as the main LoRa-based protocol, provides registration, acknowledgment services, and security aspects for LoRa-enabled IoT devices [65]. The LoRa systems operate at the ISM frequency band, between 868MHz and 900MHz (i.e., between 863 MHz and 870 MHz in Europe), depending on the location of its operation since each country uses a different frequency for LoRa technology [66]. Operation at the ISM band makes LoRa an engagement solution for the IoT and Machine-to-Machine (M2M) systems [67], and [68]. A LoRaWAN network architecture consists of a core network, gateways, and IoT devices, i.e., sensor nodes. Generally, the networks are constructed with high-performance high-cost gateways, and low-performance low-cost sensor nodes [69]. To enable low implementation complexity and high energy efficiency, LoRaWAN does not meet any specific

 doi:10.20944/preprints202306.1057.v1

medium access policy for uplink transmission. A Pure Aloha transmission policy and beyond it is favored [70]. To increase the probability of data delivery, multiple gateways can be implemented at various locations. LoRa has a sufficient range required for its implementation in remote areas [10]. Due to the convenience of deploying LoRa in remote fields, its application in the context of digital agriculture for monitoring environmental parameters is a suitable solution.

3.2. Literature study

The greater number of the research conducted on LoRa and LoRaWAN has been set on features such as coverage, range, network capacity, throughput, delay, scalability, and robustness, for instance in [51] - [56], and [71] - [75]. However, limited consideration of features such as energy consumption has been given. It is essential because many LoRa devices are not powered by the grid.

Prompted by the challenges of energy consumption, some recent works have focused on the power dissipation of sensors within wireless sensor networks [39]. Although the analyses in the majority of the proposed papers suggested to estimate the amount of energy consumed by a sensor node, LoRa technology was not included in their energy models. Thus, for instance, in [76], an energy model for ultra-low power consumption of sensor nodes was presented. However, the radio frequency module used in the study did not include LoRa technology. Another model of energy estimation was presented in [77] aimed to achieve low energy consumption of sensor nodes. In order to save energy, it was concluded that the microcontroller and the communication module must be idle as long as possible when they are not active. Although the work provides useful results, LoRa technology was not considered in the performed analysis.

Furthermore, some other studies which took LoRa communication into account did not study the optimization of the consumption of energy of LoRa sensor nodes. For instance, in [78], a comparison of LoRaWAN classes was presented and their energy consumption models were proposed. Although the obtained results are based on real measurements, the paper did not study the effects of LoRa parameters such as communication range, coding speed, and transmission power level on the total energy consumed.

The analyses presented in [57] deal with this topic to a limited measure, providing only incomplete estimates on parameters related to LoRaWAN energy efficiency. However, they did not consider the practical behavior of the hardware of the LoRaWAN device, nor the effect of the main LoRaWAN mechanism settings and parameters.

Instead, only a few works provided data relevant to the current consumption of LoRa and LoRaWAN devices, obtained from a manual or by experimental measurements [57] - [61], and [79]. Such details correspond to device states of sleep, transmission, as well as reception [69]. Although the developed models enable the characterization of lifetime and energy costs of LoRaWAN device, these models do not include, for instance, energy consumption used within the processing state of sensor units.

In addition, based on the information relevant to transmit, receive and sleep states of a LoRa/LoRaWAN device, a few analytical models of LoRa and LoRaWAN energy consumption, have been published, for example, in [57] and [62]. They include the lifetime of sensor nodes and the energy cost of data delivery. However, these models are also very basic since consideration needs to be given to several other states for a LoRa and LoRaWAN device that exist and are involved in communication. These include, for instance, a detailed calculation of time for message transmission, provided only in [80]. It is important to note that aforementioned study only aims at LoRa, and therefore does not model the use of acknowledgments and retransmission which are important mechanisms of the MAC layer defined in LoRaWAN.

Although some studies show the energy consumption of sensor nodes established on both LoRa and LoRaWAN communication, the presented values are obtained from a data table or empirically [81] - [83]. However, the studies in question did not consider an

 doi:10.20944/preprints202306.1057.v1

energy model that can thoroughly estimate and optimize the energy consumption of sensor nodes.

Considering the results of the research studies provided so far, as well as the aforementioned deficiencies in the studies, in this paper, a detailed analytical model of energy consumption of sensor nodes and energy cost of data delivery is provided. The model considers the hardware behavior and mechanisms of real LoRaWAN devices, as well as their physical and MAC layer parameters. The proposed energy consumption model is based on Class A, as the most energy-efficient LoRaWAN class. Based on the literature review, it can be concluded that this paper is among the first to specify a detailed analytical model of energy consumption and simulation of the energy cost of data delivery of sensor nodes. It considers both the real hardware behavior of LoRaWAN devices and real-case tests of data packet delivery in different specific fields of LoRa deployment scenarios. While the actual hardware behavior of LoRaWAN devices includes, for instance, their levels of power consumption in different modes of operation, the real-case tests of data packet delivery conducted in different specific LoRa field deployment scenarios enable decision making on whether a package delivery confirmation is required in a particular application scenario or not.

The defined energy model is supplemented by the optimization of LoRaWAN parameters important for the reduction of the energy consumption of sensor nodes, such as spreading factor, coding rate, and bandwidth, as well as the generated traffic volume. It is necessary to emphasize that in [39], the impact of LoRaWAN parameters such as payload size, acknowledged transmission, coding rate, spreading factor, and communication range on the sensor node consumption, is also studied. In contrast to the analyses in [39], in this paper, special emphasis is placed on the analysis of optimization of energy consumption considering different sizes of data packets which are not all very common in commercial devices and energy consumption aspects in different scenarios of LoRa network deployment.

Furthermore, unlike the analyses carried out in [66], in which the battery lifespan is calculated without the the use of acknowledgments, this paper presents the possibility of using acknowledgments to estimate the lifespan of batteries more precisely. Furthermore, the impact of deficiency of data delivery caused by degradation on the energy performance of LoRaWAN was considered. For actual analysis, the model is derived based on measurements conducted in the real testbeds. The possibility of using acknowledgments or omitting them is also analyzed, based on the results collected by real measurements, in order to select the best case for the optimization of energy consumption. In addition, the model also studies the impact of collisions on LoRaWAN energy performance.

Moreover, unlike the analyses in [33], in which the focus is placed on the optimization of the fixed LoRaWAN setup communication with only a single considered data rate, this paper analyzes the use of different available data rates to select the best method for the optimization of the energy consumption. The model considers the possibility of the use of an adaptive data transmission rate.

Finally, unlike the analyses conducted in [84] and [85], which considered large-scale LoRa network deployments with up to 100 densely distributed sensor nodes, in this paper, analyses are conducted for precision agriculture application scenarios in which deployments of up to 20 optimally distributed sensor nodes are sufficient for the monitoring of environmental parameters. Besides, unlike the energy profile used in [84] and [85], the chosen energy profile used within the simulation process is based on the estimated energy consumption [86] due to its power efficiency and application in conducted field measurements.

All procedures for modeling the energy aspects of LoRa communication processes applied in the model presented within this paper, enable a more precise assessment of the optimal combinations of parameters to achieve a reduction in the energy consumption in the selected specific use cases, whereby a special emphasis is placed on the analysis results of the optimization of energy aspects related to defining the optimal package size.

Preprints (www.preprints.org) | NOT PEER-REVIEWED | Posted: 14 June 2023 doi:10.20944/preprints202306.1057.v1

4. Energy Consumption Model of Lora Sensor Node

The energy consumption modeling process represents an essential consideration when designing sensor nodes to monitor a specific application. For most applications [87], the communicating sensors should perform the following [88]: sense events, process the local information of sensed events, and transmit packets to the access point. Each task consumes power over a given period. Therefore, an accurate energy consumption model of the sensor node is essential to estimate the sensor lifetime, as proven in [89], and [90]. Furthermore, the energy model allows the power consumption optimization of the sensor node.

In order to study the sensor node autonomy, it is necessary to model the different operating modes of the sensor node. Then, the consumed energy of each mode can be determined, and the consumption energy model can be defined.

Most of the time, the sensor node is put into sleep mode. That is a low-power mode, but the energy consumed in this mode can also impact the total energy consumption of the sensor node. The total consumed energy E_{Total} of the sensor node for one cycle is:

$$E\_{Total}=E\_{Active}+E\_{Sleep}, \quad (1)$$

where E_{Sleep} and E_{Active} represent the dissipated energy by the sensor node in the sleep mode and the total energy consumption during the active mode of the node microcontroller, respectively [89]. The duration of the sleep mode should be ≥99%, and the duration of the active mode should be ≤1% [39]. In addition, E_{Sleep} is expressed as:

$$E\_{Sleep}=P\_{Sleep}\cdot T\_{Sleep}, \quad (2)$$

where P_{Sleep} and T_{Sleep} are the power consumption and the time duration in the sleep mode, respectively [89]. The total energy consumption in active mode E_{Active} is calculated as the sum of the energy consumption used for the operation of each part of the sensor node. Therefore, it is given by the following equation [89]:

$$E\_{Active}=E\_{WU}+E\_{M}+E\_{PROC}+E\_{WUT}+E\_{Tx}+E\_{WUR}+E\_{Rx}, \quad (3)$$

where the consumed energies that should be considered are the ones for the system wake-up, data measurement, microcontroller processing, the wake-up of the transmitter, the transceiver's transmission, the wake-up of the receiver, and the reception of the transceiver, respectively [39], as presented in Figure 1.

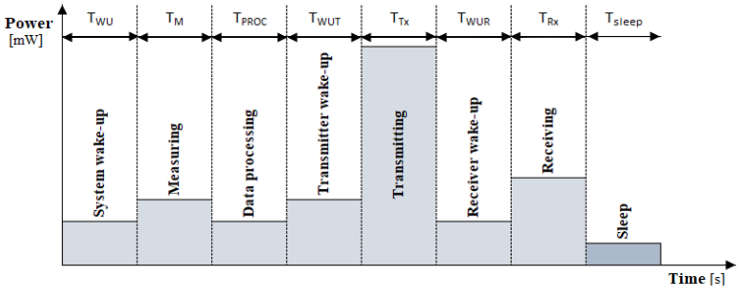

Figure 1. Energy consumption states of the sensor node.

Energy consumption in specific operating modes can be determined regarding the current consumption of LoRa/LoRaWAN transceiver modules, as declared in the specifications and affirmed by conducted measurements, presented in Table 1. As can be seen, the sleep current ranges from 0.1 μA to 34 mA. Sleep current for the hardware platforms

Table 1. Transceiver current consumption.

Transceiver	Current Consumption							
	Transmit					Receive	Sleep	References
	20 dBm	14 dBm	13 dBm	7 dBm	2 dBm			
HopeRF RFM95/96/97/98(W)	120 mA	-	29 mA	20 mA	-	11.5 mA (min. 10,.8 mA, max. 12.1 mA)	0,2 μA (max. 1 μA)	[86]

Preprints (www.preprints.org) | NOT PEER-REVIEWED | Posted: 14 June 2023 doi:10.20944/preprints202306.1057.v1

HopeRF HM-TRLR-LF/HFS	120 mA	-	35 mA	-	-	16 mA (min. 15 mA, max. 18 mA)	2 μA (max. 3 μA)	[101]
	133 mA	-	-	-	-	16.3 mA	7.7 μA	[102]
Semtech SX1276	120 mA	-	-	20 mA	-	11.5 mA (min. 10.8 mA, max. 12.0 mA)	0.2 μA (max. 1μA)	[103]
	-	-	-	-	-	14 mA	0.17 mA	[60]
	-	-	-	-	-	16.6. mA	3.7 mA	[61], [104]
	124 mA	-	-	18 mA	-	10.5 mA or 11.2 mA	0.1 μA (max. 1μA)	[105]
Semtech SX1272	-	-	-	-	-	11 mA	2 μA	[57], [106]
	-	-	-	-	26 mA	12 mA	40 μA	[58], [106]
	-	-	-	-	-	20 mA	70 μA	[59], [107]
Microchirp RN2482	-	38.9 mA	-	-	-	14.2 mA	up to 100-150 μA	[108], [109], [110], [111]
	-	48 mA	-	-	-	17.2 mA	3.4 mA	[112], [109]
	-	38.5 mA	-	-	23.9 mA	-	-	[113]
	-	-	-	-	-	46 mA	34 mA	[114]

Table 2. Transceiver power consumption.

Transmit power for the defined finite transmit power states						
Transceiver	**Transmit mode**	RFOP = +7 dBm, on RFO_LF/HF pin	RFOP = +13 dBm, on RFO_LF/HF pin	RFOP = +17 dBm, on PA_BOOST	RFOP = +20 dBm, on PA_BOOST	Reference
SX1272	**Power consumption**	95.4	95.4	297	412	[39]
RFM95/96/97/98(W)	**[mW]**	66	95.7	287	396	[86]

is up to several orders of magnitude greater than sleep current of their transceivers [105], which can be near 1 μA, or even lower than that [69]. In addition, the power consumption can be determined from the transceivers' electrical specifications under the stated supply voltage conditions.

The output power is sensitive to the power supply voltage, and their performance is typically expressed at 3.3 V [106]. For instance, the HopeRF RFM95/96/97/98(W) has the minimum output supply voltage of 2.4. V and the maximum of 3.7 V, which applies to the high power +20dBm operation [86]. According to [86], the following can be quoted:

a) Transmit mode of operation of the transceiver

In transmit mode, the power consumption, presented in Table 2, is optimized only when packet data needs to be transmitted by enabling the following blocks: RF, PLL (used for calibration of the receiver), and PA (amplifier capable of yielding RF power) [106]. The transceivers feature three different RF power amplifiers [86]. Two of these, connected to RFO_LF and RFO_HF, can deliver up to +14 dBm and are not regulated for high power efficiency [107]. The third, PA, connected to the PA_BOOST pin, can deliver up to +20 dBm via a dedicated matching network [108]. The low-frequency PA_LF covers the lower bands (up to 525 MHz), while the high-frequency PA_HF covers the upper bands (from 860 MHz). Finally, the high-power PA_HP, connected to the PA_BOOST pin, covers all frequency bands the transceiver addresses.

b) Listen mode of operation of the transceiver.

In this mode, the circuit spends most of the time in an idle state, during which only the RC oscillator is on. Then, periodically, the receiver wakes up and looks for an incoming signal. If the signal is detected, the receiver is kept on, and the data are analyzed. Otherwise, if there is no signal for a defined period of time, the receiver is switched off until the following receive period [106]. The radio stays mainly in a low power mode during the listen mode. This fact results in very low average power consumption.

c) Receive mode of operation of the transceiver

The receiver automatically restarts after a packet collision or after receiving a valid packet. In receive mode, the transceiver can detect packet collisions and restart the receiver. Collisions are detected by a sudden rise in received signal strength, detected by the RSSI. This functionality can be useful in network configurations where many asynchronous slave nodes attempt periodic communication with a single master node [106]. Depending on the application and the environment, there are certain ways to implement

 doi:10.20944/preprints202306.1057.v1

listen mode: wake on a PreambleDetect interrupt, wake on a SyncAddress interrupt, or wake on a PayloadReady interrupt [106].

According to [106], in the wake on the preamble interrupt, the sequencer polls for preamble detection. If a preamble signal is detected, the sequencer is switched off, and the circuit stays in receive mode until the user switches modes. Otherwise, the receiver is switched off until the next Rx period. When no signal is received, the circuit wakes every Timer1 + Timer2 and switches to receive mode for a time defined by Timer2. If no preamble is detected, it switches back to idle mode, i.e., sleep mode, with the RC oscillator on. If a preamble signal is detected, the sequencer is switched off [106].

According to [109], in the wake on SyncAddress interrupt, the sequencer starts for a preamble detection and then for a valid SyncAddress interrupt. If events occur, the sequencer is switched off, and the circuit stays in receive mode until the user switches modes. Otherwise, the receiver is switched off until the next Rx period. The biggest portion of the sequencer active time is spent while no signal is received. According to [86], the circuit wakes up periodically for a short time, defined by RxTimeout. The circuit is in Low Power mode for the rest of Timer1 + Timer2. However, if a preamble is detected before the RxTimeout timer ends, the circuit stays in receive mode and waits for a valid SyncAddress detection. If none is detected by the end of Timer2, the receive mode is deactivated, and the polling cycle resumes without any user intervention. However, if a valid Sync Word is detected, a SyncAddress interrupt is fired, the sequencer is switched off, and the circuit stays in receive mode, as long as the user does not switch modes.

5. Aspects of Wireless Communication Based on Lora

5.1. A. Selection of Adequate Parameters for LoRa-Based Communication

The LoRa-based access networks implemented in open spaces connect sensor nodes in different remote locations to centrally located storage and data processing servers. The range of communication is an essential parameter when considering the effectiveness of implemented solutions regarding the implementation of sensor networks in remote areas to monitor environmental and agronomic parameters. In most cases, the high data transfer rate is not so significant. However, it is necessary to ensure the energy-efficient transmission of data over relatively long distances. The parameters described hereafter affect LoRa transmission range and energy efficiency [86].

LoRa operates in the sub-GHz unlicensed frequency bands. The LoRa systems operate at the ISM frequency bands, and the carrier frequency (CF), the center frequency used for the transmission band, is 863 MHz to 870 MHz in Europe.

Moreover, according to [86], there are also some regulatory constraints in most countries on the permissible occupied bandwidth (BW). Increasing the signal bandwidth (BW) allows a higher effective data rate to be used, thereby reducing the transmission time at the expense of reduced sensitivity of the receiver. It is possible to choose between 125 kHz, 250 kHz, or 500 kHz. However, in the multi-data rate channel mode, the gateway is limited to a 125 kHz bandwidth with eight channels, even though the maximum bandwidth of LoRa is 500 kHz. Therefore, if there is a need for a high data transfer rate, the best choice is the value of 500 kHz. On the other hand, if it is necessary to achieve a long communication range, it is necessary to choose the bandwidth value of 125 kHz. The greater the bandwidth, the greater the time-on-air value, and the sensitivity of the receiver is better. However, a higher time-on-air value will also mean higher energy requirements.

The spreading factor and error correction rate allow the optimization of the trade-off between occupied bandwidth, data rate, link budget improvement, and immunity to interference.

The spread spectrum LoRa modulation is performed by representing each bit of payload information by multiple chirps of information. A chirp is a sinusoidal signal whose frequency monotonically increases (upchirp) or decreases (downchirp) [110]. According

Preprints (www.preprints.org) | NOT PEER-REVIEWED | Posted: 14 June 2023 doi:10.20944/preprints202306.1057.v1

to [110], a chirp is a pulse that sweeps from f_{Low}(−BW/2) to f_{High}(+BW/2). The number of chirps forms a symbol. For instance, if a symbol value is between 1 and 128, the number would be one of the combinations of 2^7= 128 chirps. The Spreading Factor (SF) represents the number of chirps per symbol. Its value is an integer number between 6 and 12. The values of SF from 6 to 12 represent 64, 128, 256, 512, 1024, 2048, and 4096 chirps/symbols, respectively. The greater the SF value, the more ability the receiver has to remove the noise from the signal. Thus, the greater the SF value, the more time is taken to send a packet, but a higher range will also be achieved because the receiver's sensitivity is better. For example, if the expansion factor is minimal, i.e., SF = 6, a higher speed can be achieved, but with a reduction in the possible range. The SF = 6 presents a particular use case for the highest data rate transmission possible with the LoRa modem. The spreading factor must be known in advance on both transmit and receive sides of the link, as different spreading factors are orthogonal to each other. Generally, according to the LoRaWAN specifications, the spreading factor control is limited to 6 unique spreading factors going from spreading factor 12, or the lowest data rate, to spreading factor 7, for the highest data rate. This means up to six sensor nodes can transmit data simultaneously on the same channel.

Due to interference, some of the data bits can be lost, so the error correction bits are used to recover the original lost data bits. LoRa uses Forward Error Correction (FEC) techniques to increase the robustness of radio communication links. FEC requires error correction bits, redundant bits, to be added to the data. Thus, error coding incurs a transmission overhead. Although FEC reduces the data throughput, it increases the receiver's sensitivity. LoRa defined a set of values which are referred to as Code ∈ {1, 2, 3, 4} to calculate the Coding Rate (CR) based on the following equation [111]:

$$CR = \frac{4}{4+Code} \tag{4}$$

Hence, CR = {4/5, 4/6, 4/7, 4/8}, and it denotes that every four useful bits are encoded by 5, 6, 7, or 8 transmission bits, while the overhead ratio is 1.25, 1.5, 1.75, and 2, respectively. The coding rate could maximize the data rate if fewer code bits are used. The smaller the coding rate is, the higher the time on air is to transmit data, but the prolonged data transfer time will also affect the battery consumption.

The packet header can be optionally included in the coding rate for use by the receiver. However, if more redundant bits are sent to the receiver, LoRa will consume more power. Therefore, in response to channel conditions, the coding rate and the robustness to interference can be changed.

In addition, the relationship among LoRa transmission parameters is also relevant for energy consumption. If the bandwidth of LoRa is constant, the chirp rate differs according to the SF [111]:

$$R_c = BW \cdot R_s = \frac{BW^2}{2^{SF}} \text{ [chirps/s]} \tag{5}$$

For each SF, the orthogonality of the chirp prevents interference with any other [112]. Thus, when two or more transmitters use the same channel to transmit data with different SFs simultaneously, the packets do not interfere with each other [113]. With knowledge of the key LoRa parameters [86], bandwidth, and the spreading factor, the LoRa symbol rate can be controlled:

$$R_s = \frac{BW}{2^{SF}} \quad \text{[symbols/s]} \tag{6}$$

$$SF = \log_2\left(\frac{R_c}{R_s}\right) \tag{7}$$

Moreover, depending on the SF in use, LoRa bit rate ranges [86]:

Preprints (www.preprints.org) | NOT PEER-REVIEWED | Posted: 14 June 2023 doi:10.20944/preprints202306.1057.v1

$$R_b = SF \cdot \frac{\left\lceil \frac{4}{4+CR} \right\rceil}{\left\lceil \frac{2^{SF}}{BW} \right\rceil} \cdot 1000 \ [b/s] \quad (8)$$

Data rate (DR) can also be expressed considering LoRa transmission parameters [86]:

$$DR = SF \cdot \frac{BW}{2^{SF}} \cdot CR \ [b/s] \quad (9)$$

The higher the SF and the lower the channel bandwidth, the lower the data rate is and, thus, the longer the data transmission time is, as presented in Table 3 [113].

Table 3. Maximal payload sizes.

LoRa Physical bit rate, Payload size					
Data rate (DR)	**Configuration**		**Bit rate (bps)**	**Max. MAC Payload size**	**Max. Frame Payload size**
	Modulation	Bandwidth			
0	SF12	125 kHz	250	59	51
1	SF11	125 kHz	440	59	51
2	SF10	125 kHz	980	59	51
3	SF9	125 kHz	1760	123	115
4	SF8	125 kHz	3125	230	222
5	SF7	125 kHz	5470	230	222
6	SF7	250 kHz	11000	230	222
7	FSK	50 kbps	50000	230	222
8-15			RFU		

The analysis of the effect of different values of SF and CR LoRa radio parameters on the consumed energy and range is performed in [114]. According to the presented results, the following can be concluded. When the SF value is high, the time necessary for data transmission increases. This means that the sensor node consumes more power to transmit data. The reason for setting a high SF value is to maximize the transmission range as one of the most critical factors in field deployment, as also proved in [39]. Furthermore, when the coding rate increases, the data transmission time and the consumed energy decrease. Therefore, when a long-range need to be ensured, energy consumption can be regulated by the CR factor. By increasing the CR value from 4/8 to 4/5, the energy consumption can be reduced while maintaining the maximal range enabled by the high SF parameter value [114].

5.2. Choosing the Adequate Volume of Traffic in the LoRa Network

The aim of analyzing the impact of the amount of transmitted network traffic within the network on the energy consumption for one-hop star topology scenarios is analyzed in [114], as quoted within this chapter. First, the scenario where all nodes send data at the same time interval, a typical case in rural scenarios for sending data collected from the field, is analyzed. It is concluded that node placement in star topology presents a vital determinant of sensor node lifetime. However, although adequate signal coverage of the area must be achieved, the nodes should be as close as possible to the gateway to reduce energy consumption. Moreover, regarding the energy depletion of individual nodes, it is concluded that the star topology is more suitable for application in sensor networks than the cluster topology, in which the energy of cluster head (CH) nodes is depleted the fastest. Since CH nodes are difficult to replace, this causes the loss of functionality of the entire cluster, while in the star topology, the depletion of energy of an individual node does not cause such a loss in data delivery from the area it covers with its signal. In addition, it is concluded that in scenarios where sending a more considerable amount of data is unnecessary, as in the case of monitoring the state of yield, energy savings should be achieved

 doi:10.20944/preprints202306.1057.v1

by sending an adequately determined smaller volume of data from sensors. Finally, it is concluded that significantly less energy consumption can be noted within the same time interval when sending data with higher delay, i.e., less frequently. Thus, from the presented results, applying LoRa technology is an adequate solution in IoT scenarios where fast transmission of large amounts of data is not required, as in precision agriculture. In precision agriculture, additional energy savings can be achieved by sending smaller data sets over extended periods between transmissions. Considering these conclusions, optimizing energy consumption in a LoRa network requires consideration of the optimal packet size. To save energy, sending as little total traffic as possible is necessary. Therefore, according to [115], optimizing packets to maximize information transfer in the minimum number of bits is vital. Sending the highest value information, with the right balance of redundancy, compactness, and timeliness, should provide the best results in applying a sensor network based on LoRaWAN for monitoring environmental and agronomic data essential for precision agriculture.

The LoRaWAN specification, defined for each worldwide region, provides for a maximum data payload size N. This maximum payload size varies by data rate (DR) because of the maximum on-air transmission time allowed for each regional specification. For example, for EU863-870, the maximum payload size for DR0-DR2 is 51 bytes, for DR3 is 115 bytes, for DR4-DR7 is 222 bytes, while for DR8-DR15 it is not defined [115]. If DR limits are restricted only to higher values, for instance, never below the chosen DR, this also limits how far away signals can be received, so this should be considered when choosing a packet length. Moreover, while 51 bytes in the payload in Europe may not be very restrictive, in the regions that operate in the 900MHz ISM band, the lowest DR is restricted to 11 bytes [115]. However, for all DRs other than DR0, the available maximum packet size is equal to or greater than the EU863-870 region. Therefore, if the same packet format should be used in all regions, and DR0 is chosen to be supported (since a lower DR typically means a more extended range), the maximum payload length for any packet would be 11 bytes. If the sensor node is restricted to operate above the DR0, the maximum payload becomes 51 bytes.

Since the sensors can monitor parameters related to both the environment and the state of the crops, the data in the packet payload is used to transmit measured values, for example, temperature, humidity, pressure, solar radiation, and rain. When sending data packets, it is crucial to maximize the transfer of useful information. Hence, it must be considered that the payload contents are used to maximize the transfer of useful information with minimal transmission bandwidth. Therefore, a critical aspect of data transmission planning refers to the processes for determining the necessary update rate of information to make a minimum number of samples. A reasonable sampling rate should be used to capture the original data. Moreover, for highly periodic measurements, as is the case of monitoring of majority parameters related to precision agriculture, an adequate sampling rate will result in an accurate representation of the measured values. Thus, more frequent data delivery is necessary for monitoring data related to the amount of precipitation essential for irrigation procedures, especially in the rapid occurrence of short-term storms. In these cases, it is necessary to take several samples per hour to assess the current state as accurately as possible.

It is logical to group all readings into the same packet in the case of sensors with multiple sensor elements that have synchronized measurements. In the case of group readings, bits are often arranged in registers of a fixed size, as in the example shown in the picture. However, in this case, there is an unnecessary waste of resources allocated for unused bits. For example, some sensors have 10 or 12-bit resolution, while LoRaWAN owns 8 bits or multiples slots of transmission with remaining unused bits [116], as presented in Figure 2. Therefore, optimizing the data transfer between devices is necessary to maximize the transfer of useful information in the minimum number of bytes.

Preprints (www.preprints.org) | NOT PEER-REVIEWED | Posted: 14 June 2023 doi:10.20944/preprints202306.1057.v1

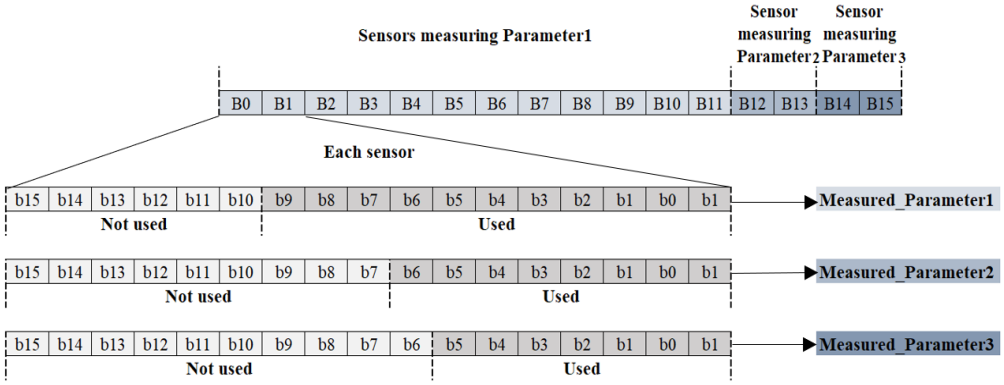

Figure 2. Grouped sensors readings.

In a group reading, the process of maximizing data transfer in the fewest bits, i.e., the process of bit packing, takes advantage of binary payload data transmission where payload bits are sent one after the other to ensure a compact flow of information. Such example of a message format as can be found at the commercially available all-in-one sensor weather stations is presented in Table 4.

Table 4. Packet payload of 11 bytes.

Packet payload format: 11-byte payload											
Measured parameter	**Type**	**Battery**	**Temperature**	**T_min**	**T_max**	**Humidity**	**Atmospheric Pressure**	**Irradiation**	**Max Irradiation**	**Rain**	**Min time between rain gauge clicks**
Bit start position	1st	3rd bit	8th bit	19th bit	25th bit	31st bit	40th bit	54th bit	64th bit	73rd bit	81sth bit
No. of bits	2	5	11	6	6	9	14	10	9	8	8
Value in binary	01	10100	10011111000	000000	000000	011011111	10011111010110	0000000001	000000000	00000000	11111111
Value in units	1	4	27.2	0	0	44.6	100990	2	0	0	255
Units	**N/A**	**V**	**°C**	**°C**	**°C**	**%**	**Pa**	**W/m2**	**W/m2**	**pulses**	**seconds**
Resolution	1	0.05	0.1	0.1	0.1	0.2	5	2	2	1	1
Max no. of values	4	32	2048	64	64	512	16384	1024	512	256	256
Min - max value	0 - 3	3 - 4.55	-100 - 104.7	0 - 6.3	0 - 6.3	0 - 102.2	50000 - 131920	0 - 2046	0 - 1022	0 - 255	0 - 255
Req min - max values	0 - 3	3 - 4.5	-50 - 80	0 - 3	0 - 3	0 - 100	60000 - 128000	0 - 1500	0 - 100	0 - 25	1 - 255
Check	**OK**	**OK**	**OK**	**OK**	**OK**	**OK**	**OK**	**OK**	**OK**	**OK**	**OK**

However, an essential aspect of bit packing is ensuring the appropriate scale and precision of the data. Many physical measurements can be compressed into smaller data bit representations, so sending more bits than required for the same data is inefficient.

For example, for transferring information about environmental temperature, the 8-bit representation instead of the 11-bit can be used. It enables the representation of a temperature range from -40^{0}C to +87.5^{0}C, sufficient to display the required temperatures with high accuracy. The same applies to other environmental parameters monitored by sensors, such as the relative humidity sensor, which can measure environmental humidity or soil moisture at different depths, and the pressure sensor or rain gauge is used to determine the maximum instantaneous rain rate. Irrigation planning based on monitoring current conditions in the environment carried out by sensor nodes represents a relevant example of the increasingly necessary application of sensor networks in precision agriculture, especially regarding the necessity of optimal water utilization, which is essential in the face of increasingly frequent water shortages. The 6-byte payload format shown in Table 5 corresponds to the optimal data set for monitoring environmental parameters

Preprints (www.preprints.org) | NOT PEER-REVIEWED | Posted: 14 June 2023 doi:10.20944/preprints202306.1057.v1

essential for the crop irrigation process, which provides the same amount of useful information as the previously shown 11-byte payload, but within the reduced packet size.

Table 5. Packet payload of 6 bytes.

Packet payload format: 6-byte payload						
Measured parameter	**Battery**	**Temperature**	**Humidity**	**Atmospheric Pressure**	**Irradiation**	**Rain**
Bit start position	1st bit	6th bit	14th bit	23rd bit	35th bit	44th bit
No. of bits	5	8	9	12	9	5
Value in binary	10100	10000110	011011111	100101101011	000000001	00000000
Value in units	4	27.0	44.6	100987	3	0
Units	**V**	**ºC**	**%**	**Pa**	**W/m2**	**pulses**
Resolution	0.05	0.5	0.2	17	3	1
Max no. of values	32	256	512	4096	512	32
Min - max value	3 - 4.55	-40 - 87.5	0 - 102.2	60000 - 129632	0 - 1536	0 - 32
Req min - max values	3 - 4.5	-50 - 80	0 - 100	60000 - 128000	0 - 1500	0 - 25
Check	**OK**	**OK**	**OK**	**OK**	**OK**	**OK**

5.3. Time on Air Constraints of Communication Based on LoRa

To optimize the overall energy consumption in the network, LoRaWAN facilitates the control of the air time and data rate [84]. To effectively manage the regulatory constraints of time on air and receiver sensitivity, it is necessary to be able to calculate the total on-the-air transmission time of a LoRa packet for a given configuration of communication parameters, i.e., spreading factor (SF), coding rate (CR) and signal bandwidth (BW), as defined hereafter. For calculating the time on air, it is convenient to define the symbol duration T_{symb}. The symbol duration of a LoRa symbol is defined as [117]:

$$T_{symb} = \frac{2^{SF}}{BW}, \quad (10)$$

This is the time taken to send chirps at the chirp rate, recalling that the bandwidth defines the chirp rate. The symbol duration is based on the spreading factor (SF) and the bandwidth (BW). Each LoRa symbol comprises 2^{SF} chirps, each covering the entire bandwidth.

Every LoRa packet consists of a preamble and data. The preamble contains only upchirps, while the data part comprises upchirps with discontinuities (the position of the discontinuities in frequency is what encodes the transmitted information). Therefore, LoRa packet duration can be calculated as the sum of the duration of the preamble and the transmitted packet. The preamble length is calculated as follows [86]:

$$T_{preamble} = (n_{preamble} + 4.25)T_{symb}, \quad (11)$$

where $n_{preamble}$ is the number of programmed preamble symbols.

The payload duration depends upon the header mode enabled, implicit (headerless) or explicit (with header) modes. The number of symbols that make up the packet payload and header are given by [86]:

$$payloadSymbNb = 8 + \max\left(ceil\left(\frac{8PL-4SF+28+16-20H}{4(SF-2DE)}\right)(CR+4), 0\right), \quad (12)$$

with the following dependencies: the number of payload bytes PL, the spreading factor SF, the header (H = 0 when header is enabled, and H = 1 when no header is present), the data rate optimization (DE = 1 when the low data rate optimization is enabled, DE = 0 when it is disabled), and the coding rate CR (from 1 to 4).

Preprints (www.preprints.org) | NOT PEER-REVIEWED | Posted: 14 June 2023 doi:10.20944/preprints202306.1057.v1

If the time on air requires reduction, and the packet length is known in advance, then the header information can be removed. The payload duration is then the symbol period multiplied by the number of payload symbols [86].

$$T_{payload} = payloadSymbNb \cdot Tsymb, \quad (13)$$

Then, the time-on-air, or packet duration, is simply the sum of the preamble and payload duration [86]:

$$T_{packet} = T_{preamble} + T_{payload}, \quad (14)$$

LoRaWAN devices must comply with the regulations imposed in the industrial, scientific, and medical (ISM) radio bands in which they operate [84]. These regulations include a limitation in the duty cycle of transmission and excited transmit power, as presented in Table 6 [118]. The duty cycle indicates the fraction of time a resource is busy. LoRaWAN enforces a per-band duty cycle limitation. In Europe, duty cycles are regulated by section 7.2.3 of the ETSI EN300.220 standard. This standard defines the following subbands and their duty cycles:

Table 6. Duty cycle restrictions.

Band	Edge frequencies		Field power	Spectrum access limitations	Bandwidth
G	863 MHz	870 MHz	+14 dBm	duty cycle < 0.1%	7 MHz
	863 MHz	870 MHz	-4.5 dBm / 100 kHz	duty cycle < 0.1%	7 MHz
	865 MHz	870 MHz	-0.8 dBm / 100 kHz	duty cycle < 0.1%	5 MHz
	865 MHz	868 MHz	+6.2 dBm / 100 kHz	duty cycle < 1%	3 MHz
G1	868.0 MHz	868.6 MHz	+14 dBm	duty cycle < 1%	600 kHz
G2	868.7 MHz	869.2 MHz	+14 dBm	duty cycle < 0.1%	500 kHz
G3	869.4 MHz	869.65 MHz	+27 dBm	duty cycle < 10%	250 kHz
G4	869.7 MHz	870 MHz	+14 dBm	duty cycle < 1%	300 kHz
G4	869.7 MHz	870 MHz	+7 dBm	duty cycle < No requirements	300 kHz

Since every radio device must comply with the regulated duty cycle limits, this applies to sensor nodes and gateways. For example, ETSI regulations limit the duty cycle over one-hour intervals, whereas LoRaWAN enforces compliance with such limitations over the interval between transmitting a message and the next one. Moreover, on The Things Network's public community network, a Fair Use Policy applies, which limits the uplink air time to 30 seconds per day per node and the downlink messages to 10 messages per day per node. If private networks are used, these limits do not apply, but the governmental and LoRaWAN limits apply.

To stay within these limits, the easiest way to do this is to calculate how much air time each packet consumes to choose a good transmit interval. For instance, as presented in Table 7, the calculator [80] is used for the chosen packet payload size (maximum of which is 51 for low data rate (SF12), up to about 222 bytes for the best conditions (SF7)), the chosen packet header size (which is at least 13 bytes for the header for regular uplinks, or a total of 23 bytes for a Join Request), the chosen coding rate (from 4/5 to 4/8, where higher values mean more overhead), the chosen number of preamble symbols (which is 8 for all regions but can be different using plain LoRa), the chosen bandwidth (which is typically 125kHz, but can be 250kHz or 500kHz), the chosen spreading factor (where "higher" means more range and better reception, but also more air time), and the chosen total air time to send the entire packet (in ms). Therefore, the calculated values include the TTN Fair Access Policy-based number of average messages/day and average messages/hour when sending all day, as well as the duty cycle-based time between the start of the next packet in the same subband.

Preprints (www.preprints.org) | NOT PEER-REVIEWED | Posted: 14 June 2023 doi:10.20944/preprints202306.1057.v1

Table 7. Maximum number of packets according to duty cycle.

Output	SF6	SF7	SF8	SF9	SF10	SF11	SF12
SF	6	7	8	9	10	11	12
DE	0	0	0	0	0	1	1
Tsym [ms]	0,5	1,0	2,0	4,1	8,2	16,4	32,8
Tpreamble [ms]	6,3	12,5	25,1	50,2	100,4	200,7	401,4
Application payload size				**51 bytes**			
payloadSymbNb [symbols]	123	103	93	83	73	83	73
Tpayload [ms]	63,0	105,5	190,5	340,0	598,0	1359,9	2392,1
Tpacket [ms]	69,2	118,0	215,6	390,1	698,4	1560,6	2793,5
TTN Fair Access Policy [messages/day]		254	139	76	42	19	10
TTN Fair Access Policy [messages/hour]		10,6	5,8	3,2	1,8	0,8	0,4
Duty cycle [s]: 0,1%	69,2	118,0	215,6	390,1	698,4	1560,6	2793,5
Duty cycle [s]: 1%	6,9	11,8	21,6	39,0	69,8	156,1	279,3
Duty cycle [s]: 10%	0,7	1,2	2,2	3,9	7,0	15,6	27,9
Application payload size				**11 bytes**			
payloadSymbNb [symbols]	53	48	43	38	33	38	33
Tpayload [ms]	27,1	49,2	88,1	155,6	270,3	622,6	1081,3
Tpacket [ms]	33,4	61,7	113,2	205,8	370,7	823,3	1482,8
TTN Fair Access Policy [messages/day]		486	265	145	80	36	20
TTN Fair Access Policy [messages/hour]		20,3	11,0	6,1	3,4	1,5	0,8
Duty cycle [s]: 0,1%	33,4	61,7	113,2	205,8	370,7	823,3	1482,8
Duty cycle [s]: 1%	3,3	6,2	11,3	20,6	37,1	82,3	148,3
Duty cycle [s]: 10%	0,3	0,6	1,1	2,1	3,7	8,2	14,8
Application payload size				**6 bytes**			
payloadSymbNb [symbols]	48	38	38	33	28	33	28
Tpayload [ms]	24,6	38,9	77,8	135,2	229,4	540,7	917,5
Tpacket [ms]	30,8	51,5	102,9	185,3	329,7	741,4	1318,9
TTN Fair Access Policy [messages/day]		583	291	161	90	40	22
TTN Fair Access Policy [messages/hour]		24,3	12,1	6,7	3,8	1,7	0,9
Duty cycle [s]: 0,1%	30,8	51,5	102,9	185,3	329,7	741,4	1318,9
Duty cycle [s]: 1%	3,1	5,1	10,3	18,5	33,0	74,1	131,9
Duty cycle [s]: 10%	0,3	0,5	1,0	1,9	3,3	7,4	13,2

As can be seen from the conducted calculations, by complying with the TTN Fair Access Policy, since more messages/hour can be sent for smaller packets, for a maximum packet size of 51 bytes, a total of 10 packets/hour cannot be exceeded. The control of the air time is done by adapting the data rate, i.e., by changing SF values. As the presented values show, the decrease in the spreading factor results in a lower air time. However, a higher air time allows the receiver to demodulate the message better.

Instead of defining a specific data rate, LoRaWAN specifies the data rate as a combination of a spreading factor and bandwidth, as presented in Table 8 [69], [119]. It can be seen that DR3 uses SF9, while DR2 uses SF10. Hence, with DR3, a double amount of data can be sent simultaneously, compared to DR2 [85]. Similarly, since the symbol time for

Preprints (www.preprints.org) | NOT PEER-REVIEWED | Posted: 14 June 2023 doi:10.20944/preprints202306.1057.v1

DR3 is half the symbol time for DR2, there will also be half the energy per bit if the same transmit power is used. Likewise, this is also true for SNR [85].

Choosing the SF parameter, which enables the highest possible transmission speed, leads to a longer battery life [80].

Despite the better range, a sensor node will consume more energy when transmitting with a higher spreading factor [84]. Therefore, in addition to modifying the spreading factor value, the transmission power can be altered to increase the range further or decrease the energy consumption.

Table 8. Data rates.

Data rate	Configuration	bits/s	Maximal application payload	Time on air per message (ms)	Messages / hour	Application bytes per hour
DR0	SF12/125kHz	250	51	2793,5	12	612
DR1	SF11/125kHz	440	51	1560,6	23	1173
DR2	SF10/125kHz	980	51	698,4	51	2601
DR3	SF9/125kHz	1760	115	676,9	53	6095
DR4	SF8/125kHz	3125	222	655,9	54	11988
DR5	SF7/125kHz	5470	222	368,9	97	21534

Considering the limitation in the duty cycle, after transmitting a message, every sensor node needs to wait Toff seconds before transmitting data again in that band (periodicity) [86]:

$$T_{off} = \frac{T_{air}}{T_{dc}} - T_{air}, \quad (15)$$

In the case of sending a message with a payload size of 51 bytes and a spreading factor of 12 while respecting a duty cycle limit of 1% (which dictates that the time for data transmit/hour is 36s), the time off is 4 minutes and 57 seconds.

Since the LoRa gateway utilizes a downlink channel allowing for a higher duty cycle and higher transmit power operation, a loss due to lowering the spreading factor can be resolved by transmitting at a higher power [85]. However, an optimal combination of energy consumption regarding limited battery life should be achieved.

To achieve a longer sensor node battery lifetime, e.g., in the order of years, the LoRaWAN nodes need batteries with greater capacity than typical button cell batteries, e.g., of AA type, but these are more expensive [69]. The results presented in [69] show that an appropriately configured LoRaWAN sensor node powered by a battery of 2400 mAh can achieve a 1-year lifetime if sending a message every 5 minutes and a theoretical lifetime of 6 years for infrequent communication. Moreover, as reported in [33], an energy consumption of 0.05–0.44 mJ and a battery lifetime between one and 13 years, respectively, are obtained for a device running on two AA batteries when transferring data from 1 to 10 times per hour.

In addition, for the chosen packet payload sizes, the calculator [120] is applied to estimate the differences in energy consumption for several types of batteries which can supply sensor nodes, as presented in Table 9. The assumptions considered are the processing power of 15 mW for 5 ms, conform reading of a sensor value per period, and the sleep mode consumption of 10µW. The worst-case results have been calculated for the usage of SF12, transmission power of +14 dBm, and with the acknowledgment in the second Rx window. The best-case results have been calculated for the usage of SF7, transmission power of +2 dBm, and with the acknowledgment in the first Rx window. As can be seen from the comparison of the collected results, a substantial energy consumption reduction can be achieved by transmitting smaller data packets.

Since sensor nodes are supplied with cell batteries upon delivery [121], purchasing the solar panel initially represents an additional cost in contrast to the sensor nodes, which

Preprints (www.preprints.org) | NOT PEER-REVIEWED | Posted: 14 June 2023 doi:10.20944/preprints202306.1057.v1

are only battery-powered. According to [121], the cost of a set of cell batteries represents approximately 12 times the cost of a cheaper sensor or approximately 2 times the cost of a more expensive sensor. Additionally, the cost of a solar panel represents 8 times the cost of a cheaper sensor, or 4/3 times the cost of a more expensive sensor. For instance, while temperature and luminosity sensors are cheaper, humidity and atmospheric pressure sensors are examples of more expensive sensors.

In the case when the duration of the battery's lifetime is short and frequent battery changes are required, the application of solar power supply represents an effective solution in the long term. However, due to the limited capacity and lifetime of batteries, they need to be replaced after a particular time, even if solar power is used.

However, in sensor networks where more sensor nodes are implemented, the energy consumption per sensor node for the exact total generated network traffic in the same period becomes lower, then when fewer sensor nodes are implemented. Thereby, the battery life per each sensor node is extended, and the battery needs to be changed less often, which demands less energy from the solar collector.

Table 9. Battery lifespan.

Application payload [bytes]	**Messages per hour**	**Configuration**	**Periodicity** T_{off} [min:s]	**Battery TTL** [year_month_week]	**Battery type**				
					AAA (Alkaline, 800mAh)	**Li-ion (260 mAh)**	**AA (Alkaline, 2500mAh)**	**Li-ion (1000 mAh)**	**Li-ion (2000 mAh)**
51	12	**SF12**/125kHz	4:57	**Worst case**	1m	1m	3m	4m	7m 3w
		SF7/125kHz	5:00	Best case	9m	9m	2y 4m 1w	2y 10m 3w	5y 9m 2w
	6	SF12/125kHz	9:57	Worst case	2m	2m	6m 1w	7m 3w	1y 3m 3w
		SF7/125kHz	10:00	Best case	1y 4m 3w	1y 5m	4y 4m 3w	5y 5m	10y 10m 1w
11	12	SF12/125kHz	4:57	Worst case	2m	2m	6m 1w	7m 3w	1y 3m 3w
		SF7/125kHz	5:00	Best case	10m 1w	10m 1w	2y 8m 1w	3y 4m	6y 8m
	6	SF12/125kHz	9:57	Worst case	4m	4m	1y 3w	1y 3m 2w	2y 7m 1w
		SF7/125kHz	10:00	Best case	1y 7m 1w	1y 7m 1w	5y	6y 2m	12y 4m 1w
6	12	SF12/125kHz	4:57	Worst case	2m 1w	2m 1w	7m 1w	9m	1y 6m
		SF7/125kHz	5:00	Best case	10m 2w	10m 2w	2y 8m 3w	3y 4m 2w	6y 9m
	6	SF12/125kHz	9:57	Worst case	4m 2w	4m 2w	1y 2m 2w	1y 5m 3w	2y 11m 3w
		SF7/125kHz	10:00	**Best case**	1y 7m 2w	1y 7m 2w	5y 3w	6y 3m	12y 6m

Preprints (www.preprints.org) | NOT PEER-REVIEWED | Posted: 14 June 2023 doi:10.20944/preprints202306.1057.v1

6.4. Unconfirmed and Confirmed Data Transfer Processes

The sensor nodes send LoRa packets to the air interface where signal propagation mode and SNR level affect the packet transmission and delivery processes, so a certain number of packets can be lost [84]. However, a part of the total packets intended for the gateway is received. Since LoRaWAN represents the Aloha-based protocol at the gateway, collisions of signals can happen [122]. Generally, the network's number of sensor nodes and gateways affects energy consumption, i.e., increasing traffic eventually causes more collisions. Therefore, LoRaWAN is affected by a high number of collisions and decreased performance in the presence of a high number of nodes [112] and [123], especially in the case of confirmed traffic [113].

The gateway can simultaneously decode the parallel transmissions performed on different SFs but on the same channel. LoRa gateway can receive up to eight packets simultaneously. These packets can be sent with different spreading factors on different channels. Due to the orthogonality of specified spreading factors, two messages encoded with different spreading factors can be demodulated concurrently without colliding.

Collisions occur if two or more packets are sent on the same channel with the same SF or if they overlap in time. In case of a collision, all collided packets are dropped. For two packets arriving at the gateway with the same SF at the same time, the gateway can decode one if it has a power greater than 6 dB above the other peak [36].

Using confirmed messages, the nodes can request acknowledgments to ensure that the gateways receive the packets successfully. It helps ensure data transmission without packet loss.

Considering possible losses in the delivery of packets, regardless of whether they are sent from sensor nodes to the network and application servers or vice versa, the sent messages can be requested to be confirmed. When sending a confirmed message, the sensor node requires that the message is acknowledged as received by the network server [131]. It expects receiving a downlink acknowledgment message in the following two receiving windows. If the acknowledgment is not received, the sensor node retransmits the same message. The same message is being retransmitted until an acknowledgment is received or until a maximum number of MAC layer transmission attempts for the message is reached. The recommended default number of attempts is eight [69]. Each transmission attempt is made in a different channel, randomly selected from the channels available in the subband. The data rate to be used is recommended to conform to the following rules. The first and second transmission attempts of a confirmed message are made using the same data rate, the third and fourth attempts use the next lower data rate (or DR0 if it was the data rate previously used), and so forth, until the eighth transmission attempt. After eight transmission attempts of the same confirmed message without acknowledgment, the MAC layer should return an error code to the application layer. Each retransmission starts after an acknowledgment timeout (ACK_TIMEOUT) period. It is initiated at the start time of the last second receive window, and is defined as a random delay between 1 and 3 seconds.

6. Evaluation and Optimization of Energy Consumption in LoRa Networks

Considering everything stated so far, a prime focus of the conducted research in this paper is on a detailed analysis of the impact of payload size on energy consumption. The selected payload sizes correspond to real-life applications related to monitoring environmental parameters used in precision agriculture. Therefore, the maximum possible payload size of 51 bytes, an average size of 11 bytes (used in most commercially available applications), and a minimum size of 6 bytes (proven optimal for the chosen precision agriculture application) are considered.

Thus, the analyses are conducted to quantify the impact of relevant LoRaWAN parameters and mechanisms on energy consumption in the scenarios in which different packet payload sizes are used.

Preprints (www.preprints.org) | NOT PEER-REVIEWED | Posted: 14 June 2023 doi:10.20944/preprints202306.1057.v1

The findings reported in [84] state that, in order to save energy, non-time-critical data can be accumulated. Furthermore, by increasing the payload size, the overhead related to header information decreases, and the number of retransmissions in a stable propagation environment reduces. For this reason, it was assumed that the grouped measurements of different parameters are sent within the same package for the analyses conducted in this paper.

Typical applications of sensor networks in precision agriculture for environmental monitoring are time-critical. Collecting current data is essential to obtain more detailed information about specific agrometeorological parameters, for example, the amount of precipitation, such as rain, in specific, more frequent periods. Hence, it is vital to provide a considerable amount of helpful information.

As opposed to the default transmission rate (λ) of 0.02 bits per second, equivalent to transmitting a 9-byte message every chosen hour, for instance, in [84], the data transmission rate is adjusted to the quantity of data that should be transmitted, i.e., to the actual packet size, as well as the packet transmitting interval. The interval is set to 10 minutes. This means the packet is transmitted every 10 minutes, so 6 packets are transmitted per hour. Moreover, the overhead data are considered for assessing the accurate transmission rate, as presented in Table 10.

Table 10. Packet payloads.

Packet Payload in Bytes	Maximal Total Packet Size in Bytes	Transmission Rate per Hour
6	14	0,19 e-3
11	19	0,25 e-3
51	59	0,79 e-3

One of the possible energy efficiency mechanisms is reducing the total volume of sent data and an adaptive data sampling process. With the less frequent data transmission, the overhead of starting and initializing a transmission is also lower. As already proven, approaches based on reducing the number of packets transmitted can improve the success rate of packet delivery. According to the TTN Fair Access Policy, for a maximum packet size of 51 bytes, a total of 10 packets/hour cannot be exceeded. Therefore, the transmission interval is set to 10 minutes, which means that data is transmitted every 10 minutes, so 6 packets are transmitted per hour. Although the sampling period of 10 minutes is more extended than the minimum of approximately 5 minutes, determined by considering duty cycle regulation, it is still short when energy savings are considered. However, it is coordinated with the necessary data related to measuring the amount of precipitation, especially in the case of short-term intense precipitation, after which the need for irrigation can be significantly reduced. The network's capacity is reduced, not only due to transmissions in the downlink but also due to the off-period time following these transmissions.

6.1. Adaptive Data Rate and Acknowledged Transmission

In [124], reliable bulk data collection in Aloha is analyzed. It is noted that in Aloha (Pure and Slotted), reliable transmission cannot be achieved in a short period, even for a low number of nodes. Aloha-based MAC protocols, such as the ones used in LoRaWAN, do not apply any mechanism to coordinate packet transmission. Each node transmits packets whenever data are available, but the duty cycle restrictions must be met. In this case, some packets are delivered while others are lost due to collisions.

The collision rate mostly depends on the transmission rate. For example, allowing the nodes to transmit in sparse intervals decreases the collisions, although it prolongs the data collection time. However, the period between transmissions has to increase considerably to make the transmission sparser and, thus, reduce the number of collisions. However, a period must be chosen in such a way as to enable the collection of an adequate

 doi:10.20944/preprints202306.1057.v1

amount of data that corresponds to the precise application scenario, as already considered when the transmission rate is selected.

Recent studies have evaluated ADR behavior in terms of convergence speed, energy consumption in different environments, and the increasing number of devices [85]. However, for determining energy efficiency, the studies [125], [126], [127] considered only the transmit power. Therefore, the energy consumption is only calculated based on the transmit power set by the device. Hence, the energy efficiency does not consider the energy required for receiving downlink messages, i.e., confirmation, or the energy consumed when the end device is in sleep mode.

In [126], the main focus is on the impact of the link distance on the ADR behavior, but it is unclear whether the simulations consider collisions and retransmissions. Finally, in [127], a fair ADR algorithm is proposed to maintain a comparable packet extraction rate for each device when the number of devices (and consequently the number of collisions) increases.

A comparison of the energy efficiency is lacking in cases in which ADR is either used or not, especially in small-scale LoRa network deployment scenarios, as, for instance, the ones used in precision agriculture.

LoRaWAN provides downlink messages to acknowledge the packet reception. Hence, if packet loss is not permitted, receiving these downlink messages and retransmitting the lost packets will also impact the energy required to transmit a packet successfully. Therefore, choosing the right combination of ADR and (un-)confirmed messages is essential when accenting energy or robustness.

For this reason, regarding losses and collisions during data transmission processes, the options to perform ADR mechanism and confirmed messages are considered in further analyses for the selected scenarios, and the impact of acknowledged transmission on the energy consumption of the sensor node is analyzed.

For analyses of energy consumption in the LoRa network in selected scenarios, the Phyton-based simulator [128] is used, which supports the ADR scheme and sending of confirmed messages [30]. The simulated preconditions for requesting packet delivery confirmation are based on packet delivery rates determined experimentally in previously analyzed scenarios.

6.2. Energy Profile

Each sensor node is characterized by an energy profile and LoRa parameters. The node's behavior is designed as specified by [129] - [132], as presented in Table 11. The energy consumption model based on LoRa, which estimates the consumed power of different states of sensor nodes, is used. The default energy profile used in the simulator is based on the energy consumption of [86] due to its energy efficiency and application in previously conducted field measurements. Therefore, the energy consumption values of the selected transceiver listed in the specifications [86] are used. Still, the simulations are not solely constrained to a single energy profile, since a comparison was made of the selected transceiver with other transceivers referenced in the literature relevant to the research area. The power consumption optimization in the selected scenarios is conducted by adopting specific power reduction settings of communication parameters. For instance, a reduction in the power consumption of the radio frequency (RF) mode is applied. As a result, it minimizes the total power consumption of sensor nodes since RF modules (for Tx and Rx) use considerable power.

During the simulation process, different energy profiles are allocated to nodes, imitating various nodes, whereby the average values of energy consumption in different states are used. The different energy states of the simulated nodes are summarized in Table 11. A similar experiment has been conducted in [84], but there are differences between the energy profile in transmit and receive modes. As can be observed from Table 11, the power states that are considered are transmit, receive, sleep, and processing, as well as waking up and setting up the radio.

Preprints (www.preprints.org) | NOT PEER-REVIEWED | Posted: 14 June 2023 doi:10.20944/preprints202306.1057.v1

Table 11. Energy profiles of the sensor nodes.

Energy profile used in the analyses						
Sensor state			**Power [86]**			**Duration (ms) [147] - [150]**
Sleep			4.95E-03 mW			-
Processing			19.14 mW			5 ms
Tx prep.			12.5 mW			40 ms
Tx	2 dBm	7 dBm	14 dBm	17 dBm	20 dBm	Eq. in [84]
	25 mW	66 mW	125 mW	287 mW	396 mW	
Wait Rx 1			4.95E-03 mW			1E3 ms
Wait Rx 2			4.95E-03 mW			1E3 - len(state Rx1)
Rx prep.			5.94 mW			3.4
Rx1			37.95 mW			air_time(DR=DR_tx)
Rx2			35.64 mW			air_time(DR=3)
Rx post proc.			5.94 mW			10.7

The simulation process assumes that all nodes have an initial transmit power of 14 dBm, which conforms to the LoRaWAN specification. This power level, which corresponds to the low-power operation mode, enables lower energy consumption than the high-power operation mode, but also sufficient signal coverage of the area, which was previously proven by field measurements. Moreover, only the operations in the channels required by the LoRaWAN specification are considered, i.e., 868.1 MHz, 868.3 MHz, and 868.5 MHz.

As already proven, optimizing the LoRa parameters such as SF, CR, and payload size are crucial in reducing the sensor node's consumed energy.

According to [129], a spreading factor SF12 should be used in the second receive window. However, in this work, a confirmed message was sent with SF10. A lower spreading factor results in a faster reception, yielding lower energy consumption at the node. The spreading factor SF10 is favored since the areas in the selected scenarios are well covered by the LoRa signal, which can be concluded according to the previously presented field measurements [66]. Moreover, a lower spreading factor results in faster data reception, which causes a lower node energy consumption. However, since the LoRa gateway handles a downlink channel by allowing for a higher duty cycle and higher transmit power operation, a loss of packets due to lowering the spreading factor can be resolved by transmitting data at higher power, as also stated in [133].

Therefore, within the simulation process, it is assumed that the downlink message scheduled for the first receive window (Rx1) uses the same frequency and data rate as the uplink messages. In the second receive window (Rx2), a fixed predefined frequency and data rate (for SF10) are used.

6.3. Coverage Range, Radio Propagation, Path Loss and Channel Variance

Regarding the analyzed sizes and range of network cells, the coverage range in rural scenarios is chosen as the highest due to a large possible width of agricultural fields. In addition, it is assumed that communication coverage decreases in urban environments with many obstacles. When choosing the range, values are chosen from previously performed field measurements from [66] of the quality of the signal.

Moreover, considering the received data on packet delivery losses from previously conducted field measurements, it can be concluded that the optimal operating range per sensor node is around 500 meters because then reliable delivery of all sent packets is enabled, even in an NLOS urban environment. Considering this fact, it is challenging to expect high-density sensor nodes in the network, for instance, in the analyses conducted in [84] where the number of sensor nodes is set to a hundred if ensuring the reliable

 doi:10.20944/preprints202306.1057.v1

transmission of data is necessary. That is why the specified range per node was considered during further analyses in individual scenarios when planning the total number of sensor nodes per coverage area in each scenario.

Wireless sensor networks with a fixed sink node often suffer from hotspots issues since sensor nodes close to the sink usually have more traffic burden to forward during the transmission process [134]. Utilizing mobile sink has been shown as an effective technique to enhance energy efficiency, network lifetime, and latency [135] and [136]. However, given the fact that the paper considers the possibility of implementing sensor nodes even on smaller agricultural lands, for instance, of 1 hectare, typical for smaller family farms, it is assumed that the use of mobile sinks is not necessary, but that a fixed arrangement of sensor nodes with the star topology within the network represents an adequate solution.

The performance of wireless sensor networks is associated with the working environment. Hence, accurate path loss modeling of a wireless communication channel must be established to represent the propagation features adequately. A path loss model can provide a precise performance evaluation of a network.

Generally, the radio channel can be characterized as a concatenation of path loss, shadowing, and multipath fading [136]. The path loss represents the average attenuation due to the distance between the transmitter and the receiver. Moreover, the shadowing represents the random fading of the received power, typically caused by the changes in the surrounding building heights. Finally, the multipath fading represents the rapid fluctuation caused by several propagation paths interfering with one another and causing significant variations with deep fades in the received power.

The simplest form of path loss is free space loss (LOS), which applies to the extreme case when nothing obstructs the propagation path. However, in practice, a propagation path is almost always obstructed (NLOS) by surrounding terrain, buildings, or the atmosphere causing refraction loss [137]. Therefore, some empirical models are used to predict path loss considering these practical effects.

A radio propagation model is an empirical mathematical formulation for the characterization of radio wave propagation as a function of frequency, distance, and other conditions. The shadowing effects caused by large-scale fading, and variations caused by small-scale fading are studied. According to the findings in the literature [138], the path loss variances are set to 0 dB for the rural LOS scenario, 5 dB for the rural NLOS scenario, 7.8 dB for the suburban NLOS scenario, and 15 dB for the urban NLOS scenario, respectively.

In order to model signal propagation scenarios in natural conditions as closely as possible through simulations, a long-distance channel model with shadowing and a COST 231 model was used. In addition, to evaluate path loss in suburban or rural (quasi-)open areas, the COST 231 path loss model was substituted into urban-to-rural and urban-to-suburban conversion.

7. Results

As stated in [85], the performance of the network and individual sensor nodes is evaluated based on the number of uniquely received packets and the mean ratio of the number of uniquely received packets on the gateway to the uniquely transmitted packets per node, i.e., the data extraction rate. This indicates how reliably the intended payload bytes are received by the gateway. Moreover, this differs from the packet delivery success ratio because it does not include retransmissions in the calculation. Hence, the main objective is that the intended payload is received by the gateway, while the number of retransmissions necessary to achieve this goal is of secondary importance. The collected results are presented and compared hereafter.

Preprints (www.preprints.org) | NOT PEER-REVIEWED | Posted: 14 June 2023 doi:10.20944/preprints202306.1057.v1

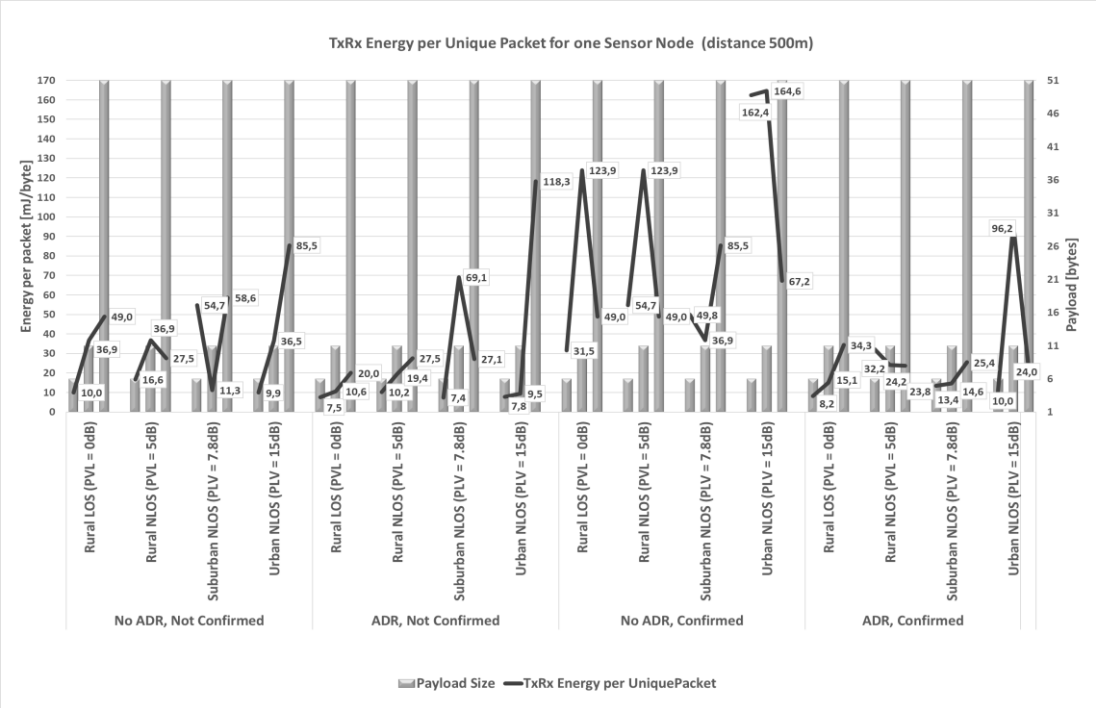

Figure 3. TxRx energy consumption per unique packet of one sensor node.

According to the presented results in Figure 3, it can be observed that the substantial energy in the transmit (Tx) and receive (Rx) states can be reduced by disabling the confirmed messages. In addition, since analyzing energy consumption optimization regarding the reduction of acknowledged transmissions, the impact of the duty cycle limit on the downlink capabilities of the gateway is also considered. The gateway cannot acknowledge all confirmed messages if only the default channels are utilized. Consequently, the number of retransmitted packages increases. Regarding the collected results for the deployed LoRaWAN sensor network scenarios, it can be concluded that the number of acknowledged frames must be minimized as much as possible to avoid capacity and energy drain.

The communication channel variance, measured in dB, concerning the average path loss, is a consequence of varying propagation characteristics of the signal in space and time. As presented, the channel dynamics significantly impact the performance of a LoRaWAN network and the energy efficiency of the nodes.

In general, according to [84] and [85], the following can be stated. First, the ADR mechanism attempts to achieve a robust signal while considering energy consumption. This is achieved by lowering the data rate when the channel conditions worsen and increasing the data rate when the SNR conditions improve.

According to the results presented in Figure 4, it is evident that ADR should be used in the analyzed scenarios since substantial energy savings can be achieved by enabling ADR. ADR reduces the energy consumption of the sensor nodes. First, it optimizes the LoRa parameters in such a way that nodes do not transmit with more power than needed. Secondly, this inherently diverges the utilized spreading factors, yielding fewer collisions. This demonstrates the importance of including ADR in assessing and optimizing transmission parameters in LPWANs to ensure a long battery life of sensor nodes.

However, ADR reacts slowly in situations with many devices or when a significant channel variance is present [84]. The current ADR mechanism is unable to adjust for the rapid channel variances. This effect is negligible if confirmed messages (i.e., retransmissions) are employed to ensure receiving each intended message. If no acknowledgments are used, the data extraction rate decreases when the channel variance increases. The

Preprints (www.preprints.org) | NOT PEER-REVIEWED | Posted: 14 June 2023 doi:10.20944/preprints202306.1057.v1

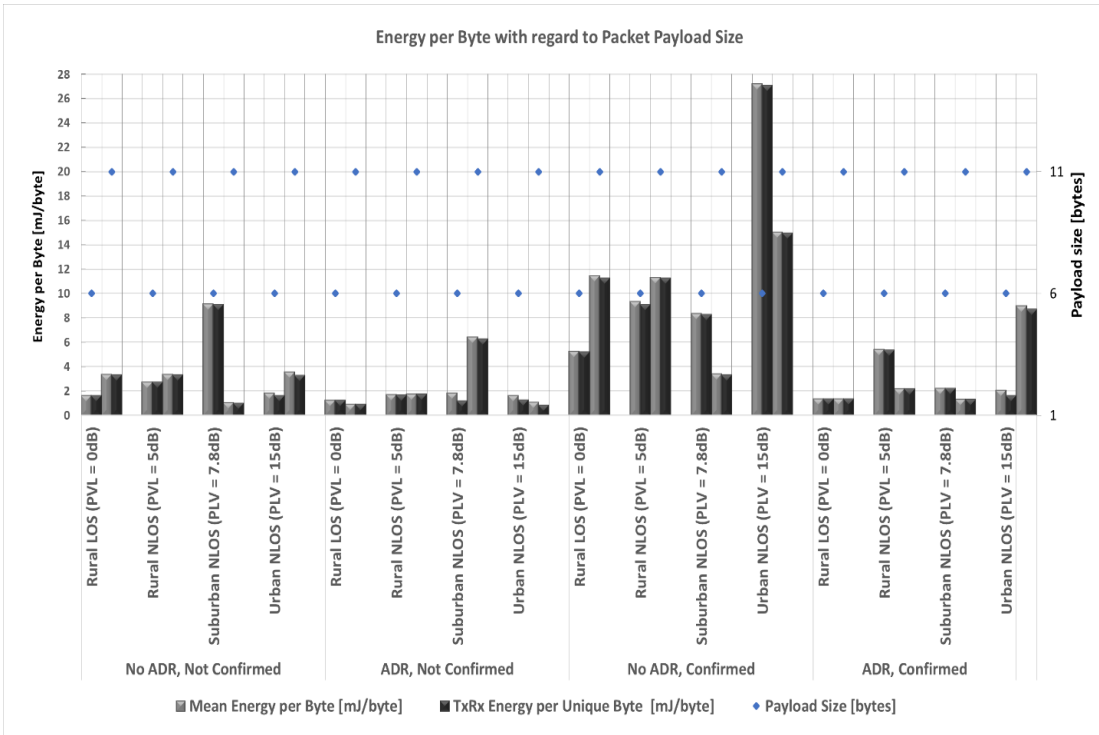

Figure 4. Consumed energy per byte for different packet payload sizes.

nodes are unable to adapt adequately to the channel. Concerning the data extraction rate, it is better not to enable an adaptive data rate when not using confirmed messages. However, this results in higher energy consumption [85].

Despite the beneficial effects of increasing the payload size, sending more bytes per packet increases the total number of bytes sent redundantly. According to [85], after receiving 20 uplink messages, the network will respond with adequate ADR parameters to accommodate non-optimal propagation. For larger payload sizes, this implies that more bytes have been sent before the LoRa parameters are adjusted to the channel. In addition, ADR changes the parameters in steps, which causes an even slower adaption to the propagation environment for larger payload sizes. This effect is notable when observing the energy consumption of nodes with a slow data transmission rate. This results in higher energy consumption. Therefore, LoRa devices should send smaller packets to adapt to the channel faster since this will reduce air time and energy consumption for packets sent with non-optimal parameters.

The energy per useful bit is a function of the maximum range and different payload sizes. The analyses conducted in [39], [84], [85] stated that with high SF values and an increase in the payload size, the energy per useful bit decreases. Also, it is stated that with low SF values, the payload variation does not substantially affect energy per helpful bit.

In extension to these analyses, the analyses carried out as part of this work consider fixed, predefined payload sizes when estimating the transmission rate values. Therefore, the corresponding transmission rate calculated is used for each scenario related to the estimation of energy consumption based on the selected packet size. The conclusions based on the obtained results fulfill those obtained in [39], [84], and [85] and indicate that, regardless of SF values, if the payload size decreases, the energy per useful bit also decreases, as well in the chosen scenarios of optimal packet sizes in bytes for the given case study.

Preprints (www.preprints.org) | NOT PEER-REVIEWED | Posted: 14 June 2023 doi:10.20944/preprints202306.1057.v1

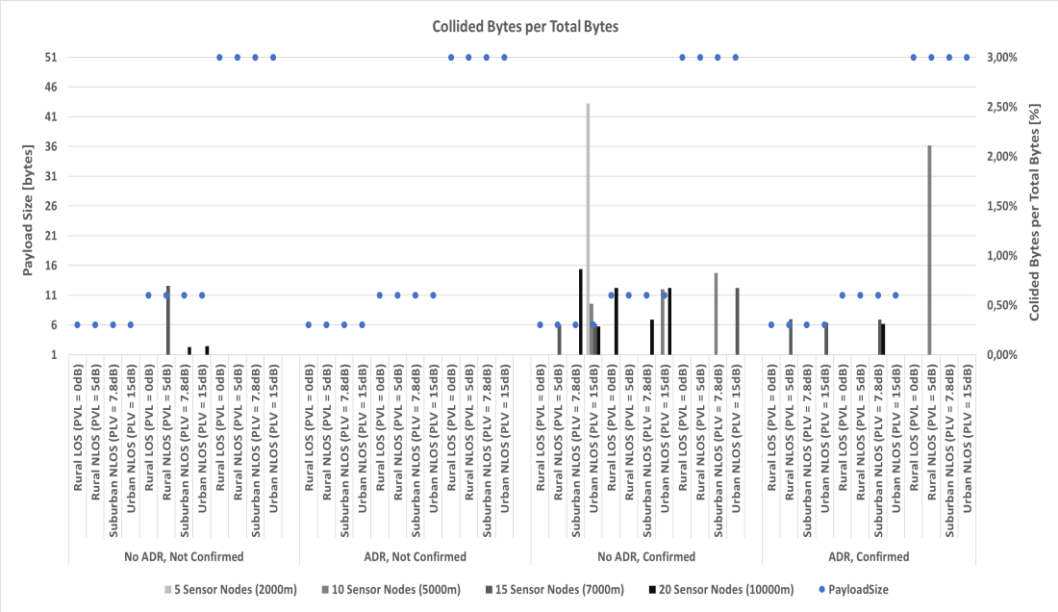

Figure 5. Percentage of bytes that collided out of the total number of bytes sent.

Delivering a large number of packets in a short time by a more significant number of nodes causes bursts of collisions, as presented in Figure 5.

In LoRaWAN, the reliability of packet delivery is achieved through the acknowledgment of packets in the downlink. However, sending confirmation increases the energy consumption in the network. Therefore, when there is a certain tolerance for packet loss, as is the case when sending not so time-critical data, for instance, data related to the state of the environmental and agronomic parameters, it is possible to omit to send confirmations. This is especially appropriate in cases of implementing sensor networks with a smaller number of nodes and sending data less often, where the frequency of possible collisions is reduced. Moreover, this is also appropriate in cases where high signal quality is ensured and there are no significant losses during packet transmissions.

Considering the stated, it can be concluded that in some cases, acknowledgments of packet delivery are not sent due to savings in energy consumption. However, to ensure the successful delivery of the amount of data needed to gain insight into the value of environmental and agronomic data necessary for crop condition assessment, it is recommended to use the packet sequence numbers nevertheless. In this way, the server could check the received traffic, and in the critical case of a more considerable difference between the sequential numbers of the two successively received packets, it can inform the sensor node that ADR should be applied and continue sending data according to its recommendations.

The LoRa network server can monitor the detailed radio information from all gateways that receive a given frame. These data include information about the gateway, extended unique identifier (EUI) of the networking devices (sensor node), server timestamp, acknowledgment flag as set by the device, frame counter (FCnt), and encrypted data payload. In addition, some extended radio information such as the radio frequency, spreading factor, bandwidth, coding rate, the gateway's Rx UTC and GPS time, and the gateway's position (latitude and longitude) can also be added. According to this information, the network server can control the sequence number of the particular packet received from the selected sensor node.

A standard comma-separated value (.CSV) file which is presented to the receiving end contains the following columns:

EUI, timestamp, FCnt, frequency, datarate, RSSI, SNR, gateway EUI, port, data

E.g.:

Preprints (www.preprints.org) | NOT PEER-REVIEWED | Posted: 14 June 2023 doi:10.20944/preprints202306.1057.v1

```
0004A30B00FFEF62,1655557243123,161,868500000,SF11 BW125 4/5,-115,-3.5,024B0BFFFF0310B2,1,693e0001bf3eb0020000ff
0004A30B00FFEF62,1655557843123,162,867500000,SF11 BW125 4/5,-102,-12.8,024B0BFFFF0310B2,1,693e4001bf3e98020000ff
0004A30B00FFEF62,1655558443123,163,867700000,SF11 BW125 4/5,-115,-2.5,024B0BFFFF0310B2,1,693e4001bf3e80020000ff
0004A30B00FFEF62,1655559043103,164,868100000,SF11 BW125 4/5,-118,-2,024B0BFFFF0310B2,1,693e4001bd3e70020000ff
0004A30B00FFEF62,1655560243103,166,868300000,SF11 BW125 4/5,-115,-7.8,024B0BFFFF0310B2,1,693e8001bd3e58000000ff
…
```

Therefore, it is evident that, based on continuous monitoring of the counter (FCnt), an insight into its changes can be gained to define an arbitrary maximum deviation from two consecutive counter values before the application of ADR is requested.

In case that the application server contains some data, for instance, about ADR usage, which it needs to transmit to a specific sleeping sensor that sends data periodically, when that sensor is a Class A device, the application server must wait for an uplink from the sensor before it can send its data [131]. The application server immediately transmits the downlink once the uplink is received. Upon receipt of the downlink, the sensor goes back to sleep. This way, even if some overhead is present, energy savings can be achieved.

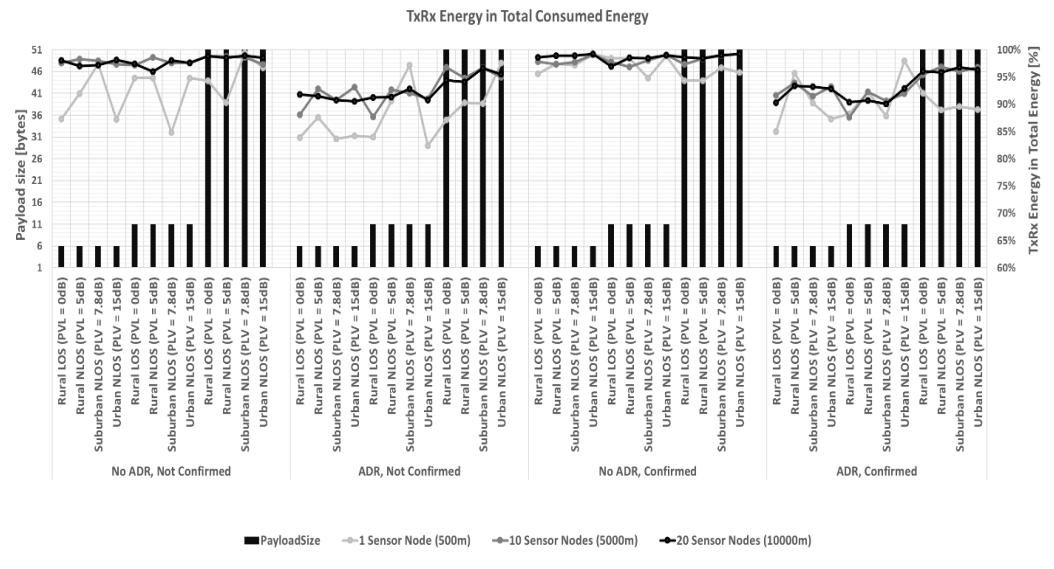

Figure 6. Percentage of TxRx energy in the total consumed energy.

Furthermore, as can be concluded from the collected results presented in Figure 6, the transmit (Tx) and receive (Rx) state energies are the most significant contributors to total energy consumption. Still, the sleep mode energy has a more significant share in the total energy if ADR is used while the confirmations are omitted, as presented in Figure 7. The results show that optimizing the LoRa parameters such as SF, CR, and payload size is a crucial element in reducing the consumed energy by the sensor node. This is also proven in [114]. The total consumed energy per useful bit is a function of the payload at different spreading factors (SF). For the more excellent value of SF, more time is taken to send a packet, so more consumed energy is needed to transmit data. Moreover, when the coding rate (CR) decreases, the time on air and, consequently, the consumed energy increases. Furthermore, there is a trade-off between the LoRaWAN communication range, the spreading factor, and the transmission power. The range is a function of SF at different transmission powers. If the SF increases, the LoRaWAN range increases as well. Moreover, the LoRaWAN range increases with increasing transmission power. It can be concluded that the theoretical maximum range that can be achieved at the determined power level is obtained with the highest SF.

Preprints (www.preprints.org) | NOT PEER-REVIEWED | Posted: 14 June 2023 doi:10.20944/preprints202306.1057.v1

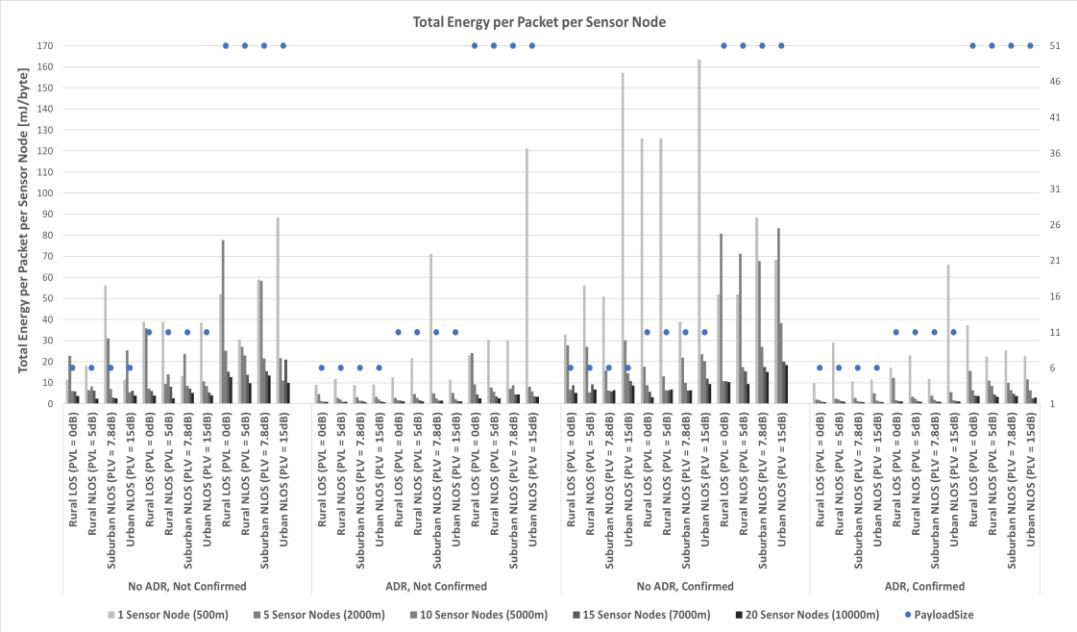

Figure 7. Total consumed energy per packet per sensor node.

8. Conclusions

This paper analyzed the energy-efficient operation of the LoRa-based wireless sensor network intended for precision agriculture. This type of sensor network may be used for crop condition monitoring by measuring essential environmental parameters such as humidity, temperature, rain gauge, and soil moisture. For achieving reliable connectivity over long distances (up to several tens of kilometers) with minimal energy consumption, LPWAN (Low Power Wide Area Network) technologies were considered. LoRa technology was selected since it was proven to be the most suitable for application within the IoT field project. Therefore, it was subjected to a more detailed analysis and testing, including simulation procedures and testing with actual equipment in real communication scenarios.

By testing LoRa communication modules in natural conditions, the results collected through analyses, simulations, and laboratory tests were compared. An optimized energy model for sensor nodes using LoRa/LoRaWAN technology was presented. It was concluded that receiving a transmission acknowledgment consumes energy, which considerably reduces the sensor node lifetime. It was shown in which way the consumed energy changes with different parameter settings.

LoRa/LoRaWAN parameters include spreading factor, coding rate, payload size, and bandwidth. Optimizing these parameters is essential to reduce the energy consumption of the sensor node.

Moreover, the difference in the analyses carried out in this paper compared to the analyses carried out in the literature so far lies in the definition of an adequate transmission rate. While the analyses carried out so far have assumed fixed values of the transmission rate, in this paper it was assumed that the transmission rate changes with each sending, considering the amount of data in the sent packets, i.e. the size of the packet. This affects the results, because in this paper it was proven that for better energy efficiency of communication, it is important to adjust the transmission speed to the actual size of the packet.

The main challenges facing the use of wireless sensor networks today are also related to security issues. While the deployment of sensor nodes makes networks vulnerable to various potential attacks, the inherent power and memory limitations of sensor nodes make conventional security solutions insufficient. For this reason, procedures have been

 doi:10.20944/preprints202306.1057.v1

proposed in the cited literature that focus not only on the optimization of the size of packets sent over the network, but also on the security issues with regard to sending of packets. In the cited literature, the lack of optimization of energy consumption is present since a fixed average transmission interval of the packets is used. This assumption considers the fact that it is not always necessary to know how long the transmission of the message will take. For this reason, in the cited literature, the transmission rate is set to the same value in all scenarios. It defines how often packets can arrive regardless of the change in the amount of data sent. Moreover, it is not strictly defined how long the transfer will last if it occurs. This increases the level of security of packet transmission in scenarios where there is a threat of packet interception. For this reason, it is best to try to send packets at random times and when it is suspected that the package is least likely to be sent so that the package can arrive at the destination with a higher probability.

Despite the aforementioned, the exchange of longer packets of information takes more time, so the process of possible packet interception is also longer. For this reason, in order to increase the security of the process of sending packets, shorter packets were selected in this paper for further analysis of their sending in different types of scenarios. Moreover, it should be noted that the data transfer procedure with a fixed transfer rate contributes to an increase in the total energy consumption. Therefore, the packet size optimization proposed in this paper was performed when the data transfer rate was adapted to the change in the amount of data being transferred, i.e. to the actual packet size. Therefore, this paper considered the case of using different values of packet transmission speed due to better optimization of energy consumption, as well as through the reduction of packet size when the security level of data transmission becomes higher.

Although the environment affects the performance of radio propagation modeling, the correlations between the energy consumption models used in the simulation process, unlike those conducted in the actual measurements, are appropriate for urban and suburban areas. In rural areas, a smaller amount of equipment is available for installation and access from sensor nodes to gateway devices. Therefore, due to the necessity of installing additional equipment in rural areas, it can be concluded that in the areas with the additional equipment installed, the signal strength may be even higher in such LOS areas than in suburban and mainly urban NLOS scenarios. This assumption is based on a real case study example as it is often necessary to implement additional equipment to enable better signal coverage and range in rural areas. However, this does not change the fact that the energy consumption ratios are equal in all simulated case study scenarios, as they would be if the simulations were carried out with propagation models more similar to pure LOS scenarios.

It was shown that there is a trade-off between the LoRaWAN communication range, the spreading factor, and the transmission power, which is essential when choosing and configuring LoRa/LoRaWAN parameters. In addition, the presented results showed that optimizing LoRa parameters, such as SF and CR, regarding the required long-range communication is crucial in reducing the consumed energy by the sensor nodes in the case study areas.

Moreover, the paper proposed a concise presentation of information in the packet payload (a 6-byte payload format, which provides the same amount of useful information as the 11-byte payload used with some commercially available devices).

In extension to some previously performed analyses (which have stated that the use of larger payloads can reduce the total energy consumption), the paper proved that, considering the reduction of energy consumption per sensor node, it is better to use smaller packets of a fixed size. From the point of view of saving energy consumption, this conclusion is based on the established minimum packet size (6-byte), which is required in the mentioned case-study scenarios in contrast to the commercially available average minimal packet size (11-byte). Furthermore, a fixed packet size allows data to be exchanged without forwarding headers when they are not needed, thereby further reducing the packet size with respect to its maximum size with the header included.

 doi:10.20944/preprints202306.1057.v1

Accordingly, one of the possible mechanisms for energy efficiency is based on reducing the total volume of sent data and an adaptive data sampling process. With less frequent data transmission, the overhead of starting and initializing a transmission is also lower. As already proved, approaches based on reducing the number of packets transmitted can improve the success rate of packet delivery. According to the TTN Fair Access Policy, for a maximum packet size of 51 bytes, a total of 10 packets/hour cannot be exceeded. Therefore, the transmission interval was set to 10 minutes, which means that data is transmitted every 10 minutes, so 6 packets were transmitted per hour. Although the sampling period of 10 minutes is more extended than the minimum possible of approximately 5 minutes determined by considering duty cycle regulation, it is still short when energy savings are considered. However, it was coordinated with the necessary data related to measuring the amount of precipitation, especially in the case of short-term intense precipitation, after which the need for irrigation can be significantly reduced. The network's capacity was reduced, not only due to transmissions in the downlink but also due to the off-time period following those transmissions.

It is important to note that, if necessary, it should always be possible to additionally adjust the number of sent packages during a specific period. For example, it is more necessary in the phase when more intensive irrigation of plants is needed in dry periods. Besides that, more intensive precipitation monitoring is possible in cases when there are greater possibilities for the occurrence of short-term weather storms, in which case it is necessary to take more frequent measurements of more intense amounts of precipitation in a short time. In contrast, it is not necessary to monitor the environmental parameters as frequently after the growing season. In such periods, the quantity of exchanged packets, as well as the size of the packet itself, can be regulated since it does not have to contain information about all environmental parameters (e.g., air pressure, the direction of the wind, etc.). Of course, a combination of different package sizes is also possible in periods when a less frequent collection of some of the environmental parameters is necessary. However, the given example of the selected minimal packet size is a more suitable solution in terms of energy saving.

It is proven that, regardless of SF values, if the payload size decreases, the energy per useful bit decreases as well.

The analyses carried out in this paper were made under the assumption of the application of star topology, which was determined to be a more energy-efficient solution compared to multi-hop topology. Nevertheless, considering the advantages of specific application examples of multi-hop topologies, future work will include the analysis of the optimization of energy consumption in multi-hop networks by exploiting various radio configurations and network topologies (e.g., the number of hops, network density, and coverage). Also, a strategy to make use of a combination of both star and multi-hop topologies will be proposed.

Acknowledgments: This work is supported by the project "IoT-field: An Ecosystem of Networked Devices and Services for IoT Solutions Applied in Agriculture" co-financed by the EU from the European Regional Development Fund within the Operational Program Competitiveness and Cohesion 2014-2020 of the Republic of Croatia.

References

1. K. Foughali, K. Fathallah, and A. Frihida, "Using cloud IoT for disease prevention in precision agriculture," Procedia Computer Science, vol. 130, pp. 575-582, 2018
2. F. Karim, F. Karim, and A. Frihida, "Monitoring system using web of things in precision agriculture," Procedia Computer Science, vol. 110, pp. 402-409, 2017
3. M. S. Farooq, S. Riaz, A. Abid, K. Abid, and M. A. Naeem, "A survey on the role of IoT in agriculture for the implementation of smart farming," IEEE Access, vol. 7, pp. 156237-156271, 2019
4. O. Elijah, T. A. Rahman, I. Orikumhi, C. Y. Leow, and N. Hindia, "An overview of Internet of Things (IoT) and data analytics in agriculture: benefits and challenges," IEEE Internet of Things Journal, vol. 5, no. 5, pp. 3758-3773, 2018
5. J. Chen and A. Yang, "Intelligent agriculture and its key technologies based on Internet of Things architecture,"

IEEE Access, vol. 7, pp. 77134-77141, 2019
6. N. Ahmed, D. De, and I. Hussain, "Internet of Things (IoT) for smart precision agriculture and farming in rural areas," IEEE Internet of Things Journal, vol. 5, pp. 4890-4899, 2018
7. M. Ayaz, M. Ammad-Uddin, Z. Sharif, A. Mansour, and E.-H. M. Aggoune, "Internet-of-Things (IoT)-based smart agriculture: toward making the fields talk," IEEE Access, vol. 7, pp. 129551-129583, 2019
8. A. Khanna and S. Kaur, "Evolution of Internet of Things (IoT) and its significant impact in the field of precision agriculture," Computers and Electronics in Agriculture, vol. 157, pp. 218-231, 2019
9. J. Wang, C. Ju, Y. Gao, A. K. Sangaiah, and G. Kim, "A PSO based Energy Efficient Coverage Control Algorithm for Wireless Sensor Networks", Computers, Materials & Continua, vol. 56, no. 3, pp. 433-446, 2018
10. K. Grgić, D. Žagar, J. Balen, and J. Vlaović, "Internet of Things in Smart Agriculture - Possibilities and Challenges", Proceedings of the International Conference on Smart Systems and Technologies, pp. 239-244, 2020
11. K. Tržec, M. Kušek, I. Podnar Žarko, "Building an Interoperable IoT Ecosystem for Data-Driven Agriculture," Proceedings of the International Conference on Smart Systems and Technologies, 2022. (More information: http://localhost:3000/dashboard/snapshot/qIGTr0auf4iLcfq7bqpsNZCCKobhtVoh)
12. Lithium-ion Battery DATA SHEET, Battery Model : LIR18650 2600mAh, EEMB Co., Ltd., Nov. 2010, Website: http://eemb.com and https://en.wikipedia.org/wiki/Lithium-ion_battery
13. Srbinovska, M.; Dimcev, V.; Gavrovski, C. Energy Consumption Estimation of Wireless Sensor Networks in Greenhouse Crop Production. In Proceedings of the 17th International Conference on Smart Technologies, Ohrid, Macedonia, 6–8 July 2017; IEEE: Ohrid, Macedonia, 2017; pp. 870–875.
14. Zou, T.; Lin, S.; Feng, Q.; Chen, Y. Energy-efficient control with harvesting predictions for solar-powered wireless sensor networks. Sensors 2016, 16, 53.
15. J. Wang, Y. Gao, C. Zhou, R. S. Sherratt, and L. Wang, "Optimal Coverage Multi-Path Scheduling Scheme with Multiple Mobile Sinks for WSNs", Computers, Materials & Continua, vol. 62, no. 2, pp. 695-711, 2020
16. Fourie, C.; Bhatt, D.; Silva, B.; Kumar, A.; Hancke, G. A solar-powered fish pond management system for fish farming conservation. In Proceedings of the International Symposium on Industrial Electronics (ISIE), Scotland, UK, 19–21 June 2017; pp. 2021–2026.
17. Nguyen, T.-D.; Thanh, T.T.; Nguyen, L.-L.; Huynh, H.-T. On the Design of energy Efficient Environment Monitoring Station and Data Collection Network Based on Ubiquitous Wireless Sensor Networks. In Proceedings of the 2015 IEEE RIVF International Conference on Computing & Communication Technologies-Research, Innovation, and Vision for the Future (RIVF), Cần Thơ, Vietnam, 25–28 January 2015; pp. 163–168.
18. Ilie-Ablachim, D.; Pătru, G.C.; Florea, I.-M.; Rosner, D. Monitoring device for culture substrate growth parameters for precision agriculture: Acronym: Monisen. In Proceedings of the 2016 15th RoEduNet Conference: Networking in Education and Research, Bucharest, Romania, 7–9 September 2016; IEEE: Bucharest, Romania, 2016; pp. 1–7.
19. C. Kamienski, J. P. Soininen, M. Taumberger et al., "Smart water management platform: IoT-based precision irrigation for agriculture," Sensors, vol. 19, no. 2, p. 276, 2019.
20. A. D. Boursianis, M. S. Papadopoulou, A. Gotsis et al., "Smart irrigation system for precision agriculture - the ARETHOU5A IoT platform," IEEE Sensors Journal, vol. 21, no. 16, Article ID 17539, 2021.
21. M. Ayaz, M. Ammad-Uddin, Z. Sharif, A. Mansour and E. M. Aggoune,Internet-of-Things (IoT)-Based Smart Agriculture: Toward Making the Fields Talk, IEEE Access 2019, Vol. 7, pp. 129551–129583.https://doi.org/10.1109/ACCESS.2019.2932609
22. Mesas-Carrascosa, F.; Santano, D.V.; Meroño, J.; de la Orden, M.S.; García-Ferrer, A. Open source hardware to monitor environmental parameters in precision agriculture. Biosyst. Eng. 2015, 137, 73–83.
23. Azaza, M.; Tanougast, C.; Fabrizio, E.; Mami, A. Smart greenhouse fuzzy logic based control system enhanced with wireless data monitoring. ISA Trans. 2016, 61, 297–307.
24. Aiello, G.; Giovino, I.; Vallone, M.; Catania, P.; Argento, A. A decision support system based on multisensory data fusion for sustainable greenhouse management. J. Clean. Prod. 2018, 172, 4057–4065.
25. M. A. Akkas, and R. Sokullu, "An IoT-based greenhouse monitoring system with Micaz motes," Procedia Computer Science, vol. 113, pp. 603-608, 2017
26. C. A. Gonzalez-Amarillo, J. C. Coralles-Munoz, M. A. Mendoza Moreno, A. M. G. Amarillo, A. F. Hussein, N. Arunkumar, and G. Ramirez-Gonzalez, "An IoT-based traceability system for greenhouse seedling crops," IEEE Access, vol. 6, pp. 67528-67535, 2018
27. F. Karim, F. Karim, and A. Frihida, "Monitoring system using web of things in precision agriculture," Procedia Computer Science, vol. 110, pp. 402-409, 2017
28. J. M. Talavera, L. E. Tobon, J. A. Gomez, M. A. Culman, J. M. Aranda, D. T. Parra, L. A. Quiroz, A. Hoyos, and L. E. Garreta, "Review of IoT applications in agro-industrial and environmental fields," Computers and Electronics in Agriculture, vol. 142, pp. 283-297, 2017
29. J. Doshi, T. Patel, S. K. Bharti, "Smart farming using IoT, a solution for optimally monitoring farming conditions," Procedia Computer Science, vol. 160, pp. 746-751, 2019
30. The project "IoT-field: An Ecosystem of Networked Devices and Services for IoT Solutions Applied in Agriculture" the EU Operational Program Competitiveness and Cohesion of the Republic of Croatia, 2014-2020
31. R. P. Centelles, F. Freitag, R. Meseguer, and L. Navarro "Beyond the Star of Stars: an Introduction to Multi-Hop and Mesh for LoRa and LoRaWAN", IEEE Pervasive Computing, vol. 20, pp. 63-72, 2021

32. Yonghua Song, Jin Lin, Ming Tang, Shufeng Dong, An Internet of Energy Things Based on Wireless LPWAN, Engineering, Volume 3, Issue 4, 2017, Pages 460-466, ISSN 2095-8099, https://doi.org/10.1016/J.ENG.2017.04.011.
33. L. Chettri, "A comprehensive survey on Internet of Things (IoT) toward 5G wireless systems," IEEE Internet of Things Journal, vol. 7, pp. 16-32, 2020
34. U. Raza, P. Kulkarni, and M. Sooriyabandara, "Low power wide area networks: an overview," IEEE Communications Surveys & Tutorials, vol. 19, pp. 855-873, 2017
35. K. Mekki, E. Bajic, F. Chaxel, and F. Meyer, "A comparative study of LPWAN technologies for large-scale IoT deployment," ICT Express, vol. 5, pp. 1-7, 2019
36. R. S. Sinha, Y. Wei, and S.-H. Hwang, "A survey on LPWA technology: LoRa and NB-IoT," ICT Express, vol. 3, pp. 14-21, 2017
37. J. P. S. Sundaram, W. Du, and Z. Zhao, "A survey on LoRa networking: research problems, current solutions, and open issues," IEEE Communications Surveys & Tutorials, vol. 22, pp. 371-388, 2020
38. J. Xu, J. Yao, L. Wang, Z. Ming, K. Wu, and L. Chen, "Narrowband Internet of Things: evolutions, technologies, and open issues," IEEE Internet of Things Journal, vol. 5, pp. 1449-1462, 2018
39. T. Bouguera, J.-F. Diouris, J.-J. Chaillout, R Jaouadi, and G Andrieux., "Energy Consumption Model for Sensor Nodes Based on LoRa and LoRaWAN" Sensors 2018, no. 7: 2104. https://doi.org/10.3390/s18072104
40. Kolobe, L., Sigweni, B. and Lebekwe, C. K. (2020) Systematic literature survey: applications of LoRa communication. International Journal of Electrical and Computer Engineering (IJECE), 10 (3), 3176-3183. http://doi.org/10.11591/ijece.v10i3.pp3176-3183.
41. Muhammad Ayoub Kamal, Muhammad Mansoor Alam, Aznida Abu Bakar Sajak, Mazliham Mohd Su'ud, "Requirements, Deployments, and Challenges of LoRa Technology: A Survey", Computational Intelligence and Neuroscience, vol. 2023, Article ID 5183062, 15 pages, 2023. https://doi.org/10.1155/2023/5183062
42. Zehua Sun, Huanqi Yang, Kai Liu, Zhimeng Yin, Zhenjiang Li, and Weitao Xu. 2022. Recent Advances in LoRa: A Comprehensive Survey. ACM Trans. Sen. Netw. 18, 4, Article 67 (November 2022), 44 pages. https://doi.org/10.1145/3543856
43. Idris, Sadiq, Thenuka Karunathilake, and Anna Förster. 2022. "Survey and Comparative Study of LoRa-Enabled Simulators for Internet of Things and Wireless Sensor Networks" Sensors 22, no. 15: 5546. https://doi.org/10.3390/s22155546
44. Chenning Li and Zhichao Cao. 2022. LoRa Networking Techniques for Large-scale and Long-term IoT: A Down-to-top Survey. ACM Comput. Surv. 55, 3, Article 52, 36 pages. https://doi.org/10.1145/3494673
45. J. P. Shanmuga Sundaram, W. Du and Z. Zhao, "A Survey on LoRa Networking: Research Problems, Current Solutions, and Open Issues," in IEEE Communications Surveys & Tutorials, vol. 22, no. 1, pp. 371-388, Firstquarter 2020, doi: 10.1109/COMST.2019.2949598.
46. Raychowdhury, A., Pramanik, A. (2020). Survey on LoRa Technology: Solution for Internet of Things. In: , et al. Intelligent Systems, Technologies and Applications. Advances in Intelligent Systems and Computing, vol 1148. Springer, Singapore. https://doi.org/10.1007/978-981-15-3914-5_20
47. A. Ikpehai et al., "Low-Power Wide Area Network Technologies for Internet-of-Things: A Comparative Review," in IEEE Internet of Things Journal, vol. 6, no. 2, pp. 2225-2240, April 2019, doi: 10.1109/JIOT.2018.2883728.
48. S. Devalal and A. Karthikeyan, "LoRa Technology - An Overview," 2018 Second International Conference on Electronics, Communication and Aerospace Technology (ICECA), Coimbatore, India, 2018, pp. 284-290, doi: 10.1109/ICECA.2018.8474715
49. Ertürk, Mehmet Ali, Muhammed Ali Aydın, Muhammet Talha Büyükakkaşlar, and Hayrettin Evirgen, 2019. "A Survey on LoRaWAN Architecture, Protocol and Technologies" Future Internet 11, no. 10: 216. https://doi.org/10.3390/fi11100216
50. Haxhibeqiri, Jetmir, Eli De Poorter, Ingrid Moerman, and Jeroen Hoebeke. 2018. "A Survey of LoRaWAN for IoT: From Technology to Application" Sensors 18, no. 11: 3995. https://doi.org/10.3390/s18113995
51. Adelantado, F.; Vilajosana, X.; Tuset-Peiro, P.; Martinez, B.; Melia, J. Understanding the limits of lorawan. IEEE Communications Magazine, 2017, Available online: https://arxiv.org/pdf/1607.08011
52. Augustin, A.; Yi, J.; Clausen, T. A study of LoRa: Long range & low power networks for the Internet of Things. Sensors 2016, 16, 1466.
53. G. H. Derevianckine, A. Guitton, O. Iova, B. Ning and F. Valois, "Opportunities and Challenges of LoRa 2.4 GHz," in IEEE Communications Magazine, 2023, doi: 10.1109/MCOM.010.2200566.
54. Petajajarvi, J.; Mikhaylov, K.; Pettissalo, M.; Janhunen, J.; Iinatti, J. Performance of a low-power wide-area network based on LoRa technology: Doppler robustness, scalability, and coverage. Int. J. Distrib. Sens. Netw. 2017, 13, 1–16.
55. C. Milarokostas, D. Tsolkas, N. Passas and L. Merakos, "A Comprehensive Study on LPWANs With a Focus on the Potential of LoRa/LoRaWAN Systems," in IEEE Communications Surveys & Tutorials, vol. 25, no. 1, pp. 825-867, Firstquarter 2023, doi: 10.1109/COMST.2022.3229846
56. Haxhibeqiri, J.; Van den Abeele, F.; Moerman, I.; Hoebeke, J. LoRa Scalability: A Simulation Model Based on Interference Measurements. Sensors 2017, 17, 1193.
57. Kim, B.; Hwang, K. Cooperative Downlink Listening for Low-Power Long-Range Wide-Area Network. Sustainability 2017, 9, 627.
58. Mahmoud, M.S.; Mohamad, A.A. H. A Study of Efficient Power Consumption Wireless Communication Techniques/ Modules for Internet of Things (IoT) Applications. Adv. Intern. Things 2016, 6, 19–29.

59. Bor, M.; Roedig, U. LoRa Transmission Parameter Selection. In Proceedings of the 13th IEEE International Conference on Distributed Computing in Sensor Systems (DCOSS), Ottawa, ON, Canada, 5–7 June 2017.
60. Magno, M.; Aoudia, F.A.; Gautier, M.; Berder, O.; Benini, L. WULoRa: An energy efficient IoT end-node for energy harvesting and heterogeneous communication. In Proceedings of the IEEE Design, Automation & Test in Europe Conference & Exhibition, Lausanne, Switzerland, 27–31 March 2017; pp. 1528–1533.
61. Dongare, A.; Hesling, C.; Bhatia, K.; Balanuta, A.; Pereira, R.L.; Iannucci, B.; Rowe, A. OpenChirp: A Low-Power Wide-Area Networking architecture. In Proceedings of the IEEE International Conference on Pervasive Computing and Communications Workshops (PerCom Workshops), Kona, HI, USA, 13–17 March 2017; pp. 569–574.
62. I. Cheikh, R. Aouami, E. Sabir, M. Sadik and S. Roy, "Multi-Layered Energy Efficiency in LoRa-WAN Networks: A Tutorial," in IEEE Access, vol. 10, pp. 9198-9231, 2022, doi: 10.1109/ACCESS.2021.3140107.
63. Sornin, N.; Luis, M.; Eirich, T.; Kramp, T.; Hersent, O. LoRaWAN Specification; Version V1.0.2; LoRa Alliance: Beaverton, OR, USA, 2016.
64. LoRaWAN™ Certified Products. Available online: https://www.lora-alliance.org/certified-products
65. LoRa Alliance Technical Committee. LoRaWAN™ 1.0.3 Specification. 2018. Available online: lora-alliance.org/sites/default/files/2018-07/lorawan1.0.3.pdf
66. J. Spišić, A. Pejković, M. Zrnić, V. Križanović, K. Grgić, and D. Žagar, "LoRaWAN Parameters Optimization for Efficient Communication," Proceedings of the International Conference on Smart Systems and Technologies, 2022
67. Oliveira, R.; Guardalben, L.; Sargento, S. Long Range Communications in Urban and Rural Environments. In Proceedings of the IEEE Symposium on Computers and Communications Conference (ISCC), Heraklion, Greece, 3–6 July 2017.
68. Elodie, M.; Mickael, M.; Roberto, G.; Andrzej, D. Comparison of the Device Lifetime in Wireless Networks for the Internet of Things. IEEE Access 2017, 5, 7097–7113
69. L. Casals, B. Mir, R. Vidal, and C. Gomez. 2017. "Modeling the Energy Performance of LoRaWAN" Sensors 2017, no. 10: 2364. https://doi.org/10.3390/s17102364
70. G. Yapar, T. Tugcu and O. Ermis, "Time-Slotted ALOHA-based LoRaWAN Scheduling with Aggregated Acknowledgement Approach," 2019 25th Conference of Open Innovations Association (FRUCT), Helsinki, Finland, 2019, pp. 383-390, doi: 10.23919/FRUCT48121.2019.8981533.
71. J. Wang, H. Han, H. Li, S. He, P. K. Sharma, and L. Chen, "Multiple Strategies Differential Privacy on Sparse Tensor Factorization for Network Traffic Analysis in 5G", IEEE Transactions on Industrial Informatics, vol. 18, no. 3, pp. 1939-1948, 2022
72. Augustin, A.; Yi, J.; Clausen, T. A study of LoRa: Long range low power networks for the Internet of Things. Sensors 2016, 16, 1466.
73. Haxhibeqiri, J.; Van den Abeele, F.; Moerman, I.; Hoebeke, J. LoRa Scalability: A Simulation Model Based on Interference Measurements. Sensors 2017, 17, 1193.
74. Nolan, K.E.; Guibene, W.; Kelly, M.Y. An evaluation of low power wide area network technologies for the Internet of Things. In Proceedings of the IEEE International of Wireless Communications and Mobile Computing Conference (IWCMC), Paphos, Cyprus, 5–9 September 2016; pp. 440–444.
75. Lucas Eduardo Ribeiro, Davi Wei Tokikawa, João Luiz Rebelatto, Glauber Brante, Comparison between LoRa and NB-IoT coverage in urban and rural Southern Brazil regions, Annals of Telecommunications, Issue 11-12/2020
76. Mochammad Haldi Widianto, Arief Ramadhan, Agung Trisetyarso, Edi Abdurachman. Energy saving on IoT using LoRa: a systematic literature review, International Journal of Reconfigurable and Embedded Systems (IJRES), Vol. 11, No. 1, March 2022, pp. 25~33, doi: 10.11591/ijres. v11.i1. pp25-33
77. Mare, S.; Vladimir, D.; Cvetan, G. Energy Consumption Estimation of Wireless Sensor Networks in Greenhouse Crop Production. In Proceedings of the IEEE EUROCON 17th International Conference on Smart Technologies, Ohrid, Macedonia, 6–8 July 2017; pp. 870–874.
78. Phui, S.C.; Johan, B.; Chris, H.; Jeroen, F. Comparison of LoRaWAN Classes and their Power Consumption. In Proceedings of the IEEE Symposium on Communications and Vehicular Technology (SCVT), Leuven, Belgium, 14 November 2017.
79. Casals, L.; Mir, B.; Vidal, V.; Gomez, C. Modeling the Energy Performance of LoRaWAN. Sensors 2017, 17, 2364.
80. http://forum.thethingsnetwork.org
81. Neumann, P.; Montavont, J.; Noël, T. Indoor deployment of low-power wide area networks (LPWAN): A LoRaWAN case study. In Proceedings of the IEEE 12th International Conference onWireless and Mobile Computing, Networking and Communications (WiMob), New York, NY, USA, 17–19 October 2016; pp. 2–9.
82. Mikhaylov, K.; Petajajarvi, J. Design and implementation of the plug-play enabled flexible modular wireless sensor and actuator network platform. Asian J. Control 2017, 19, 1393–1411.
83. Johnny, G.; Patrick, V.T.; Jo, V.; Hendrik, R. LoRa Mobile-To-Base-Station Channel Characterization in the Antarctic. Sensors 2017, 17, 1903
84. G. Callebaut, G. Ottoy and L. van der Perre, "Cross-Layer Framework and Optimization for Efficient Use of the Energy Budget of IoT Nodes," Proceedings of the IEEE Wireless Communications and Networking Conference, pp. 1-6, 2019
85. G. Callebaut, G. Ottoy and L. V. d. Perre, "Optimizing Transmission of IoT Nodes in Dynamic Environments," 2020 International Conference on Omni-layer Intelligent Systems, pp. 1-5, 2020
86. RFM95/96/97/98(W) v1.0 & v2.0 - Low Power Long Range Transceiver Module, https://www.hoperf.com/modules/lora/RFM95.html

87. Rao Muzamal Liaqat, Philip Branch, and Jason But. 2023. LoRa Based Linear Network Applications, Design Considerations and Open Challenges: A Review. In Proceedings of the 20th ACM Conference on Embedded Networked Sensor Systems (SenSys '22). Association for Computing Machinery, New York, NY, USA, 913–917. https://doi.org/10.1145/3560905.3568111
88. Jayantha Nayak, Manoj P, Uday J, 2022, A Review on LoRa Transmission, International Journal of Engineering Research and Technology (IJERT) ICEI – 2022 (Volume 10 – Issue 11)
89. on LoRa and LoRaWAN. https://hal.archives-ouvertes.fr/hal-01828769/document
90. M. S. Philip and P. Singh, "Energy Consumption Evaluation of LoRa Sensor Nodes in Wireless Sensor Network," 2021 Advanced Communication Technologies and Signal Processing (ACTS), Rourkela, India, 2021, pp. 1-4, doi: 10.1109/ACTS53447.2021.9708341.
91. HopeRF HM-TRLR-LF/HFS Series 100 mW. Available online: http://www.hoperf.com/upload/rf/HM-TRLR-S_Series_english_.pdf
92. Conus, G.; Lilis, G.; Zanjani, N.A.; Kayal, M. An event-driven low power electronics for loads metering and control in smart buildings. In Proceedings of the Second International Conference on IEEE Event-Based Control, Communication, and Signal Processing (EBCCSP), Krakow, Poland, 13–15 October 2016; pp. 1–7.
93. Semtech SX1276. Available online: https://www.semtech.com/products/wireless-rf/lora-connect/sx1276
94. LoRaBug. Available online: https://github.com/OpenChirp/LoRaBug
95. Semtech SX1272. Available online: https://www.semtech.com/products/wireless-rf/lora-connect/sx1272
96. LoRaWAN Multitech mDot. Available online: http://www.multitech.com/documents/publications/datasheets/86002171.pdf
97. NetBlocks XRange. Available online: https://www.netblocks.eu/xrange-sx1272-lora-datasheet/
98. Mendívil, L.J. Comparación de Soluciones Basadas en LPWAN e IEEE 802.15.4 Para Aplicaciones de Salud Móvil ("m-Health"). Master's Thesis, Centro de Investigación Científica y de Educación Superior de Ensenada, Ensenada, Mexico, 2017.
99. Microchip RN2483 LoRa Mote. Available online: http://www.microchip.com/DevelopmentTools/ProductDetails.aspx?PartNO=dm164138
100. Microchip RN2483. Available online: http://ww1.microchip.com/downloads/en/DeviceDoc/50002346A.pdf
101. Errata Microchip RN2483. Available online: http://ww1.microchip.com/downloads/en/DeviceDoc/80000689A.pdf
102. Neumann, P.; Montavont, J.; Noël, T. Indoor deployment of low-power wide area networks (LPWAN): A LoRaWAN case study. In Proceedings of the IEEE 12th International Conference on Wireless and Mobile Computing, Networking and Communications (WiMob), New York, NY, USA, 17–19 December 2016; pp. 1–8.
103. Petajajarvi, J.; Mikhaylov, K.; A.; Yasmin, R.; Hämäläinen, M.; Iinatti, J. Evaluation of LoRa LPWAN Technology for Indoor Remote Health and Wellbeing Monitoring. Int. J. Wirel. Inf. Netw. 2017, 24, 153–165.
104. Mikhaylov, K.; Petäjäjärvi, J. Design and implementation of the plug&play enabled flexible modular wireless sensor and actuator network platform. Asian J. Control 2017, 19, 1392–1412.
105. Extraordinary optical transmission - Wikipedia. https://en.wikipedia.org/wiki/Extraordinary_optical_transmission
106. ISL067 ISL067R Operational Description SX1276-7-8.book Invisible Systems. https://fccid.io/ZWZ-ISL067/Operational-Description/operational-description-2326556
107. Application of LoRa Protocol on Arduino - Principle and Code Analysis (1) https://blog.csdn.net/weixin_39584176/article/details/104814971
108. SX1272/73 - doczz.net. https://doczz.net/doc/7947188/sx1272-73
109. 7.3.2. Wake on SyncAddress Interrupt. Semtech SX1236. https://manualzz.com/doc/o/15k5bf/semtech-sx1236-fsk-transceiver-datasheet-7.3.2.--wake-on-syncaddress-interrupt
110. Chirp Spread Spectrum (CSS) - IoT ONE. https://www.iotone.com/term/chirp-spread-spectrum-css/t110
111. Mohammed Alenezi, Kok Keong Chai, Yue Chen, Shihab Jimaa, Ultra-dense LoRaWAN: Reviews and challenges, First published: 01 June 2020, https://ietresearch.onlinelibrary.wiley.com/doi/10.1049/iet-com.2018.6128
112. Bor, M.C.; Roedig, U.; Voigt, T.; Alonso, J.M. Do LoRa Low-Power Wide-Area Networks Scale? In Proceedings of the 19th ACM International Conference on Modeling, Analysis and Simulation of Wireless and Mobile Systems (MSWiM '16), Valletta, Malta, 13–17 November 2016; pp. 59–67.
113. https://www.thethingsnetwork.org/forum/t/how-to-find-maximum-packet-size/25321/2
114. V. Križanović, D. Ćaćić, K. Grgić, and D. Žagar, "Energy Efficiency of LoRa based Wireless Sensor Networks for Environmental Monitoring and Precision Agriculture," Proceedings of the Eighteenth Advanced International Conference on Telecommunications AICT 2022, June 2022, Porto, Portugal
115. LoRa Developer Portal, https://lora-developers.semtech.com/documentation/technical-documents, [retrieved: July, 2022]
116. Ana I. Pereira, Florbela P. Fernandes, João P. Coelho, João P. Teixeira, Maria F. Pacheco, Paulo Alves, Rui P. Lopes, Optimization, Learning Algorithms and Applications: First International Conference, OL2A 2021, Bragança, Portugal, July 19–21, 2021, Revised Selected Papers, Communications in Computer and Information Science, Springer Nature, 2021.
117. Stewart, Shania, Ha H. Nguyen, Robert Barton, and Jerome Henry. 2019. "Reducing the Cost of Implementing Filters in LoRa Devices" Sensors 2019, no. 18: 4037. https://doi.org/10.3390/s19184037
118. https://witekio.com/fr/blog-fr/lorawan-a-dedicated-iot-network/
119. https://lora-developers.semtech.com/documentation/tech-papers-and-guides/the-book/packet-size-considerations
120. https://dramco.be/tools/lora-calculator/

121. Libelium products and pricing catalogue, https://manualzz.com/doc/8165880/libelium-products-and-pricing-catalogue
122. Suciu, I., Pacho, J.C., Bartoli, A., Vilajosana, X. (2018). Authenticated Preambles for Denial of Service Mitigation in LPWANs. In: Montavont, N., Papadopoulos, G. (eds) Ad-hoc, Mobile, and Wireless Networks. ADHOC-NOW 2018. Lecture Notes in Computer Science, vol 11104. Springer, Cham. https://doi.org/10.1007/978-3-030-00247-3_19
123. Georgiou, O.; Raza, U. Low Power Wide Area Network Analysis: Can LoRa Scale? IEEE Wirel. Commun. Lett. 2017, 6, 162–165.
124. Zorbas, D.; Caillouet, C.;Abdelfadeel Hassan, K.; Pesch, D. Optimal Data Collection Time in LoRa Networks—A Time-Slotted Approach. Sensors 2021, 21, 1193.https://doi.org/10.3390/s21041193
125. V. Hauser and T. Hegr, "Proposal of adaptive data rate algorithm for lorawan-based infrastructure," in 2017 IEEE 5th International Conference on Future Internet of Things and Cloud (FiCloud), 2017, pp. 85–90.
126. A. Peruzzo and L. Vangelista, "A power efficient adaptive data rate algorithm for lorawan networks," in 2018 21st International Symposium on Wireless Personal Multimedia Communications (WPMC), 2018, pp. 90–94.
127. K. Q. Abdelfadeel, V. Cionca, and D. Pesch, "A fair adaptive data rate algorithm for lorawan," CoRR, vol. abs/1801.00522, 2018. [Online]. Available: http://arxiv.org/abs/1801.00522
128. G. Callebaut, "LoRaWAN Network Simulator," doi: 10.5281/zenodo.1217124.
129. LoRa™ Modulation Basics, Semtech Std., 2015, aN1200.22. [Online]. Available: https://www.semtech.com/uploads/documents/an1200.22.pdf
130. SX1272/3/6/7/8: LoRa Designer's Guide, Semtech Std., 2013, aN1200.13. [Online]. Available: https://www.semtech.com/uploads/documents/LoraDesignGuide STD.pdf
131. LoRaWAN™ 1.0.3 Specification, LoRa Alliance, 2018, https://lora-alliance.org/wp-content/uploads/2020/11/lorawan1.0.3.pd
132. SX1272/3/6/7/8: LoRa Modem Low Energy Consumption Design, Semtech Std., 2013, aN1200.17. [Online]. Available: https://www.semtech.com/uploads/documents/LoraLowEnergyDesign STD.pdf
133. A.-I. Pop, U. Raza, P. Kulkarni, and M. Sooriyabandara, "Does bidirectional traffic do more harm than good in LoRaWAN based LPWA networks?" arXiv preprint arXiv:1704.04174, 2017
134. J. Wang, Y. Cao, B. Li, H. Kim, and S. Lee, "Particle Swarm Optimization based Clustering Algorithm with Mobile Sink for WSNs", Future Generation Computer Systems, vol. 76, pp. 452-457, 2017
135. D. Praveen Kumar, Tarachand Amgoth, Chandra Sekhara Rao Annavarapu, "Machine learning algorithms for wireless sensor networks: A survey", Information Fusion, Volume 49, 2019, Pages 1-25, ISSN 1566-2535, https://doi.org/10.1016/j.inffus.2018.09.013.
136. M. Wagrowski, "Understanding UMTS Radio Network Modelling, Planning and Automated Optimization, Theory and Practice [Book Review]," in IEEE Communications Magazine, vol. 44, no. 12, pp. 30-30, Dec. 2006, doi: 10.1109/MCOM.2006.273096.
137. J. Wang, Yu Gao, X. Yin, F. Li, and. H.-J. Kim, "An Enhanced PEGASIS Algorithm with Mobile Sink Support for Wireless Sensor Networks", Wireless Communications & Mobile Computing, vol. 2018, Article ID 9472075, 2018
138. Yahia Zakaria, Jiri Hosek and Jiri Misurec, "Path Loss Measurements for Wireless Communication in Urban and Rural Environments", American Journal of Engineering and Applied Sciences, 2015, 8 (1): 94.99, DOI: 10.3844/ajeassp.2015.94.99